Cerebral Cortex March 2009;19:658-674
doi:10.1093/cercor/bhn114
Advance Access publication July 16, 2008

Entorhinal Cortex Inhibits Medial Prefrontal Cortex and Modulates the Activity States of Electrophysiologically Characterized Pyramidal Neurons In Vivo

Ornella Valenti and Anthony A. Grace

University of Pittsburgh, Department of Neuroscience, Psychiatry and Psychology, Pittsburgh, PA 15260, USA

The prefrontal cortex receives multiple inputs from the hippocampal complex, which are thought to drive memory-guided behavior. Moreover, dysfunctions of both regions have been repeatedly associated with several psychiatric disorders. Therefore, understanding the interconnections and modulatory interactions between these regions is essential in evaluating their role in behavior and pathology. The effects of entorhinal cortex (EC) stimulation on the activity of identified medial prefrontal cortex (mPFC) pyramidal neurons were examined using single-unit extracellular recordings and sharp-electrode intracellular recordings in anesthetized rats. Single-pulse electrical stimulation of EC induced a powerful inhibition in the majority of mPFC neurons examined during extracellular recording. Intracellular recording showed that EC stimulation evoked a complex synaptic response, in which the greater proportion of neurons exhibited excitatory postsynaptic events and/or a short lasting and a prolonged inhibitory postsynaptic response. Furthermore, stimulation of EC selectively produced an augmentation of the bistable up–down state only in the type 2 regular spiking neurons and in a subclass of nonintrinsic bursting neurons. Taken together, these data suggest that the potent inhibition observed following EC stimulation may mask a direct excitatory response within the mPFC which markedly potentiates the bistable states in a select subpopulation of mPFC pyramidal neurons.

Keywords: bistable states, electrophysiology, GABA, intracellular recordings, in vivo, pyramidal

In the past several years, the prefrontal cortex has received substantial interest due to the key role it plays in a wide variety of task ranging from learning and memory (Goldman-Rakic 1995; Laroche et al. 2000; Dash et al. 2007) to the regulation of emotional states (Herman et al. 1996; LaBar and Cabeza 2006; Quirk et al. 2006; Sotres-Bayon et al. 2006). These multifaceted activities are believed to be driven by multiple interconnections between the medial prefrontal cortex (mPFC) and specific limbic and midbrain structures as well as sensory association cortices in the parietal and temporal lobes (Sesack et al. 1989; Conde et al. 1995; Vertes 2004; Gabbott et al. 2005). Based on these data, the PFC is positioned to provide a functional interface between cognitive and limbic regions in processing information and modulating goal-directed behavior, emotion, and memory (Horvitz 2000; Simons and Spiers 2003; Kesner and Rogers 2004; McDonald et al. 2004; Ridderinkhof et al. 2004; Goto and Grace 2005; Sakagami and Pan 2007).

Pyramidal neurons recorded in the rat mPFC in vivo are known to exhibit a bistable state, in which the membrane shifts from a hyperpolarized, inactive membrane potential (down state) to a plateau depolarized (up) state from which spikes are triggered (Steriade et al. 1993a, 1993b; Contreras et al. 1996; Sanchez-Vives and McCormick 2000; Cossart et al. 2003; Shu et al. 2003). The presence of such states in mPFC is well-established (Cowan and Wilson 1994; Amzica and Steriade 1995, 1998; Branchereau et al. 1996). These up and down states are believed to be generated via interactions among neocortical neurons (Destexhe and Pare 1999; Destexhe et al. 2001; Steriade et al. 2001; DeFelipe et al. 2002) and have been proposed to serve as a gate for afferent drive (O'Donnell and Grace 1995). The bistable state of mPFC pyramidal neurons is also thought to be influenced by afferent inputs. In particular, a very high percentage of pyramidal neurons receive a complex synaptic influence from the hippocampus (HPC) (Jay et al. 1989; Jay and Witter 1991), exhibiting a combination of excitatory and inhibitory effects (Laroche et al. 1990; Degenetais et al. 2003). Although the up state had been shown to be dependent on an intact hippocampal afferent system (O'Donnell et al. 2002), stimulation of the CA1/subiculum portion of the HPC failed to change the onset or frequency of occurrence of up and down states in any of the 3 different classes of mPFC pyramidal neurons examined (Degenetais et al. 2003). Moreover, studies show that projections from the ventral tegmental area to the mPFC may prolong the up states in mPFC pyramidal neurons; however, this effect is restricted to neurons that already showed spontaneously generated up states (Lewis and O'Donnell 2000). The mPFC is also known to receive projections from another temporal lobe region, the entorhinal cortex (EC), which has received substantial interest in recent years because of its potential contribution in regulating memory-guided events and its possible role in the pathophysiology of several psychiatric disorders including mood disorders and schizophrenia (Nasrallah et al. 1997; Kalus et al. 2005; Meunier et al. 2006; Witter and Moser 2006). Anatomical studies have demonstrated widespread direct projections from the EC to mPFC in rats (Sarter and Markowitsch 1985; Swanson and Kohler 1986; Insausti et al. 1997) which arise from a restricted group of neurons located in the more lateral and caudal parts of the EC, and close to the border of the rhinal sulcus (Sarter and Markowitsch 1985). Retrograde tracing studies show that these projections arise in distinct regions, with layers V and VI of the EC innervating primarily the prelimbic mPFC and layer III innervating the infralimbic mPFC (Insausti et al. 1997). These afferents are nonreciprocal, and typically innervate the superficial layers of the PFC (Insausti et al. 1997; Delatour and Witter 2002). Despite the potential role of the hippocampal complex and the EC in regulating memory-guided events and emotional state in the mPFC (Hasselmo 2005; Vertes 2006),

there have been a paucity of studies regarding the functional impact of EC projection system on neuronal activity within the mPFC.

Using in vivo single-unit extracellular and sharp-electrode intracellular recordings in rats, we examined the manner by which the EC affects mPFC pyramidal neuron activity. Thus, this study provides the first evidence that the EC not only potently inhibits mPFC pyramidal neuron activity, but also is capable of providing a neuron cell type-specific drive of the bistable state. Together, these interactions are positioned to effectively gate information flow within the mPFC.

Materials and Methods

All animals used in these studies were handled in accordance with the guidelines outlined in the National Institute of Health Guide for the Care and Use of Laboratory Animals. The Institutional Animal Care and Use Committee of the University of Pittsburgh approved all studies described in this paper, and experimental protocols were in accordance with all applicable guidelines regarding the care and use of animals.

Subjects and Surgery

Experiments were performed in 280–400 g male Sprague–Dawley rats (Hilltop, Scottdale, PA). Animals were housed in pairs upon arrival in a temperature and humidity controlled environment with lights maintained on a 12-h light/dark cycle and food and water available ad libitum. On the day of the experiment, a rat was anesthetized with an intraperitoneal injection of 8% chloral hydrate (400 mg/kg) and placed in a stereotaxic device (David Kopf Instruments, Tujunga, CA). For the duration of the surgery and the experiment, supplemental doses of chloral hydrate were administered intraperitoneally as necessary to maintain anesthesia and suppress hindlimb compression reflex. Body temperature was monitored with a rectal probe and maintained at ~37 °C with a heating pad (FHC, Bowdoinham, ME). An incision was made on the scalp to expose the skull, burr holes were drilled in the skull overlying the mPFC (site of recording), the EC or the perirhinal cortex (PrC; sites of stimulation), and the ventral HPC (vHPC; site of drug administration); and the dura overlying these areas was resected. Coordinates for these areas were determined using the stereotaxic atlas of Paxinos and Watson (2007), as follows (in mm from bregma): mPFC = +2.8 to +3.4 anteroposterior (AP), +0.5 to +0.8 lateral (L), −2.5 to −5.5 ventral from skull surface (V); EC = −6.3AP, −1.65L, −8.9V in a 30° angle; PrC = −6.3AP, −1.65L, −8.9V in a 35° angle; vHPC = −5.9AP, +5L, −5V.

Single-Unit Extracellular Recording

In vivo single-unit extracellular recordings were performed from prelimbic and infralimbic mPFC pyramidal neurons, as previously described (Floresco and Grace 2003; Laviolette et al. 2005). Single-barrel glass microelectrodes were constructed from borosilicate glass capillary tubing (2 mm outer diameter, World Precision Instruments, Sarasota, FL) using a vertical microelectrode puller (Narishige, Tokyo, Japan), the electrode tips were broken back under microscopic control against a glass rod. The electrode was then filled with 2 M NaCl in 2% pontamine sky blue dye using a nonmetallic Microfill syringe needle (World Precision Instruments, Inc) and Whatman Puradisc Syringe filter (Whatman Schleicher & Schuell, Florham Park, NJ). The impedance of those electrodes, measured in situ, ranged between 7 and 12 MΩ which, in accordance with Jung and colleagues (Jung et al. 1998), is adequate for isolating action potential discharge from individual pyramidal neurons. The recording electrode was lowered slowly from the prelimbic to infralimbic portions of the mPFC employing a hydraulic micromanipulator (model 640; David Kopf Instruments, Tujunga, CA), until a spontaneously active neuron was detected. Neurons with spike durations of >1.1 ms and regular spiking (RS) pattern with firing rate <5 Hz were classified as pyramidal neurons, based on previously established criteria (Jung et al. 1998; Tierney et al. 2004; Tseng et al. 2006; Floresco and Tse 2007; McCracken and Grace 2007). Signals from the recording electrode were amplified by a headstage connected to the preamplifier before being fed into a window discriminator/amplifier (1000x gain, 100- to 4000-Hz band pass, Fintronics Inc., Orange, CT), with low cutoff of 50 Hz (for neuron observation/classification) or 200 Hz (for neuron recording), and a high cutoff of 16 kHz. Signals were also fed into an audio monitor (AM8; Grass Instruments, Quincy, MA) and displayed on an oscilloscope (model 2120, BK Precision, Yorba Linda, CA) for real time monitoring, as well as to a custom-designed digital acquisition system (Neuroscope, Brian Lowry).

Sharp-Electrode Intracellular Recording

Sharp-electrode intracellular recordings were performed in vivo from 50 mPFC neurons of 37 rats, as previously described (O'Donnell and Grace 1995; Lavin and Grace 2001). Borosilicate glass single-barrel capillaries (1 mm outer diameter, 0.58 mm inner diameter; World Precision Instruments, Inc) were pulled using a horizontal Flaming-Brown micropipette puller (model P-80/PC; Sutter Instruments, Novato, CA). The electrodes were filled with a solution containing 3 M KAc in 2% biocytin (Sigma-Aldrich, St Louis, MO); the impedance measured in situ ranged between 65 and 90 MΩ. The Grass stimulator connected to the external drive of the intracellular recording amplifier (model IR-283; Neuro Data Instruments, New York, NY) was used to control current delivery to the electrode. Intracellular current was injected via an active bridge circuit integral to the preamplifier, and the amplitude of this current was monitored using custom-design computer software, Neuroscope; any variation in electrode balance was immediately compensated by adjusting the bridge. Electrode potentials were corrected for the liquid junction potential and monitored in real time using an oscilloscope or Neuroscope, a multimeter (model 179A TRMS multimeter; Keithley, Cleveland, OH) and with an audio monitor. Square steps of current (0.6 nA, 150 ms), constantly delivered at 2-Hz frequency, were employed during the cell-searching process. Cell penetration was defined as stable when the cell exhibited a resting membrane potential of at least −55 mV, fired action potentials with ⩾50 mV amplitude, exhibited membrane capacitance charge in response to hyperpolarizing current injection and fired a train of spikes in response to injection of depolarizing current steps. Data were collected for neurons that had been defined as stable when these electrophysiological properties were maintained for a minimum period of 5 min. Consistent with a previous study (Degenetais et al. 2002), all mPFC neuron types were identified and classified into 3 main subtypes accordingly to their spontaneous activity (baseline), the amplitude histogram obtained from baseline, and their response to depolarizing current steps. The spontaneous firing frequency, the membrane voltage and its coefficient of variation, and amplitude histogram were calculated from 3 min recording epochs. In addition, intracellular injections of depolarizing current were employed in order to characterize and classify each pyramidal neuron. Specifically, each step consisted of 400-ms duration increasing amplitude current pulses, that is, +0.3, +0.5, +0.7, 1 nA, that were repeated 4–5 times; both the number of evoked spikes and the pattern of discharge were evaluated in order to classify each pyramidal neuron recorded. Current–voltage relationships (IV plots) were established by injecting 200-ms square-wave current pulses with increasing intensity, from −1.2 nA up to suprathreshold positive current by 0.2 nA steps. Voltage responses were measured at the steady-state membrane potential response, calculated from the average of 5 responses, and plotted versus current injection amplitude. Input resistance (R_i) was calculated from a regression of the current injection/membrane potential response relationship. Membrane time constants (τ) were obtained by injecting a −0.2 nA hyperpolarizing current pulse and measuring the time required for the membrane potential to reach 63% of the maximal deflection. Data were fed from the amplifier to a desktop computer, then monitored and collected for off-line analysis. At the end of all experimental manipulations, the electrode was withdrawn from the cell and the extracellular electrode tip potential was assessed; membrane potential measurements were then corrected accordingly.

Electrical Stimulation of the EC and PrC

Electrical stimulation of the lateral EC or PrC was delivered by using a bipolar concentric electrode (NEX-100; Rhodes Medical Instrument,

Inc., Summerland, CA) connected to a stimulus isolation unit (PSIU6; Grass Instruments Co.) in series with a Grass Instruments S88FS stimulator (Grass Medical Instruments, Quincy, MA). The stimulus timing was driven by the software Neuroscope and stimulation of EC obtained by delivering a pulse of 0.5 mA current, 250 μs duration, repeated at least 100 times at 0.5-Hz frequency. Typically, mPFC neuron afferents were first stimulated using low current amplitudes (0.1–0.5 mA); however, in most of our experiments, a second set of 100 single-pulse stimuli was delivered to EC at 1 mA. This second set of stimuli allowed investigation of the effects of EC stimulation in those neurons in which consistent responses could not be obtained at low stimulus intensities. Responses of mPFC pyramidal neurons to EC stimulation were recorded starting at 200-ms prestimulus and continuing for 750- to 900-ms poststimulus. Data thus obtained were plotted in peristimulus time histograms (PSTHs), and the effect of EC stimulation on mPFC pyramidal neuron activity was thereby evaluated and measured.

Following evaluation of responses to single pulses for neuron type identification, the response to "train stimulation" of the EC was evaluated. Train stimulation consisted of a single 20 Hz train, 100 pulses for a duration of 5 s; data were collected for 1-min prestimulus, during 5 s of maintained stimulation, and then for 5 min following the train. In a separate set of experiments the responses of mPFC neurons to single-pulse stimulation of the PrC was tested using the same stimulation parameters, to evaluate whether the responses recorded were contaminated by current spread to adjacent structures.

The parameters of EC stimulation employed during intracellular recordings were similar to those used for extracellular recordings. Following neuron classification and recording 3 min of baseline activity, 250-μs single-pulse stimuli were delivered to the lateral EC in order to examine the effects of EC stimulation on pyramidal neuron activity and intrinsic membrane proprieties. Stimulation was initiated using lower amplitude currents, and then tested at progressively higher current intensities in 3-min sets at each current intensity (0.5 and 1 mA). In another set of experiments the EC was stimulated only at one amplitude of current, either 0.5 or 1 mA, in order to exclude any cumulative or synergic effects on membrane potentials. During EC stimulation, mPFC neuronal activity was typically recorded continuously for 3 min, with a total of 18 stimuli delivered at each current amplitude tested. These modifications of the protocol, with respect of the one employed in extracellular recordings, allowed observation of both the effects on evoked postsynaptic potentials and the effects on membrane voltage oscillation. Evoked excitatory postsynaptic potentials (EPSPs) as well as 2 types of inhibitory postsynaptic potentials (IPSPs), that is, a short-duration IPSP (sIPSP) and a prolonged IPSP (pIPSP), were detected during EC stimulation. The membrane potential dependence of the evoked postsynaptic responses was analyzed by delivering 4–5 stimuli to the EC during membrane hyperpolarization via intracellular current injection and averaging the resultant responses. In this set of experiments, the EC was stimulated at 0.5 mA; however, in order to evaluate the effects of current intensity on the evoked postsynaptic event, in some experiments single-pulse stimulation was delivered at higher current intensities. Prior to each sweep of EC stimulation, a 50-ms hyperpolarizing current step was delivered to test the neuron input resistance. In a few experiments (n = 2 for each pyramidal neurons subtype) train stimulation, consisting of 5 or 10 pulses, 10 ms ISI repeated every 3 s for 3 min, was delivered to compare the elicited response with those evoked by single stimuli.

Drug Administration

A possible contribution of the HPC → fornix output pathway was also evaluated by chemical inactivation of the vHPC (CA1 and ventral subiculum), which was achieved by local injection of lidocaine (Sigma-Aldrich). A 2% lidocaine solution was premade, and then aliquoted and stored at −20 °C. Lidocaine was administered directly in the vHPC by microinfusion, according to the coordinates from the rat Atlas (Paxinos and Watson 2007). Stainless steel guide cannulae (26 gauge, Plastic One, Roanoke, VA) were implanted into vHPC and 0.5 μL of drug was infused through a 26-gauge microinfusion injector (Plastic One) connected via a polytetrafluoroethylene tubing (Small Parts Inc, Miami Lakes, FL) to a 5-μL glass syringe (model 88011; Hamilton Company, Reno, NV). The speed of administration was controlled with a BAS syringe pump (model MD-1001; Bioanalytical Systems, Inc, W. Lafayette, IN) to administer 0.2 μL of lidocaine per minute.

Statistics and Data Analysis

Data were collected and monitored simultaneously on-line using the custom-designed computer software, Neuroscope, and a data acquisition board interface (Microstar laboratory, Bellevue, WA). Electrophysiological analysis of mPFC pyramidal neuron activity both during baseline and EC stimulation was performed off-line using Neuroscope. All data are reported as mean ± SEM. Individual comparisons were made using one-way ANOVA, or Kruskal–Wallis one-way ANOVA on Ranks, where appropriate, or Student's t tests. All statistics were performed using the software SigmaStat (Systat Software, Inc.).

In order to quantify and statistically compare the effect of EC stimulation, PrC stimulation, and lidocaine application on mPFC pyramidal neuron activity during extracellular recordings, 3 different parameters were defined, which also helped in characterizing mPFC pyramidal neuron responses to stimulation of the EC (Floresco and Tse 2007): 1) onset of response, 2) duration of response, and 3) percent excitation or inhibition of firing. Because of the low firing rate of mPFC pyramidal neurons, only neurons showing reliable prestimulus neuronal activity were included in the analysis. In accordance with previously established criteria (Ishikawa and Nakamura 2003; Floresco and Tse 2007), analysis of the PSTH enabled identification of several types of responses to EC stimulation, including a pure inhibitory response, a short-latency excitation followed by an inhibitory response, or no response. A neuron was classified as "inhibited" by EC stimulation only if it displayed a complete cessation of action potential discharge for at least 50 ms. The "onset" of an inhibitory response was defined as the time between the stimulus artifact and last spike before a complete cessation of neuronal activity which lasted for at least 50 ms. The "duration" of inhibitory response was measured as previously defined (Ishikawa and Nakamura 2003; Floresco and Tse 2007) and its value calculated as the time interval between the last spike occurring in a 200-ms period after stimulation and the recovery of baseline firing activity. Lastly, a third criterion, the percent inhibition, was employed, which was calculated with the same equation used by Floresco and Tse (2007). Neurons were classified as excited if EC stimulation evoked a cluster of spikes typically showing a Gaussian pattern of distribution and appeared as increased probability of spike firing. The latency of excitation, calculated from stimulus onset to evoked spike initiation, was consistent with orthodromic activation; that is, the evoked spikes occurred within the first 50 ms after stimulus artifact, and the evoked spikes occurred at a variable latency. All neurons exhibiting any other type of short-latency response which did not fall into this definition were therefore excluded from this study. The duration of an excitatory response was defined as the time interval between the first spike and the last spike of a cluster which occurred within the first 50 ms from stimulus artifact. Both duration and percent of excitation were calculated by comparing the last 50 ms of prestimulus firing rate with the first 50 ms following EC stimulation. The 3 previously described criteria were applied also to characterize the effects of train stimulation on mPFC pyramidal neuron activity. Thus, the percent inhibition or excitation was calculated by comparing the changes in firing rate occurring 10-s pre- and post-train stimulation, with the 10-s value being the minimal duration of inhibition observed from the termination of the train.

In all intracellular recordings, characterization of the neurons, the existence of bistable membrane activity, and the effects of EC stimulation on the membrane activity of mPFC pyramidal neurons were evaluated employing previously established criteria (O'Donnell and Grace 1995; Lavin and Grace 2001). Changes of the intrinsic membrane proprieties were measured by comparing the first minute of baseline activity of mPFC neurons with the last minute of recording during EC stimulation.

Electrode Marking and Histology

At the end of all experimental protocols, rats were prepared for histological verification of recording and stimulation sites. Both for extracellular and intracellular recording experiments, stimulation sites

were marked by an electrical deposit of iron, which was obtained by passing a 10 s, 1 mA positive single step current pulse through the stimulating electrode. Microinfusion locations were determined by the location of the injector tip and, in some cases, injection of pontamine sky blue dye via the cannula.

In rats used for extracellular experiments, the recording site was marked via electrophoretic ejection of pontamine sky blue dye from the tip of the recording electrode (30 μA constant current; for 30–50 min). In rats used for intracellular recordings, mPFC pyramidal neurons were injected with biocytin via application of depolarizing pulses (~0.5 nA, 300 ms; for 20–30 min) through the recording electrode. At the end of recordings, the rats were deeply anesthetized and perfused transcardially through the ascending aorta with ice-cold saline, followed by fixative solution consisting of 4% paraformaldehyde in phosphate buffered saline (PBS).

Rats were then decapitated, the brains removed and placed in 8% paraformaldehyde solution with potassium ferricyanide (Sigma-Aldrich), which reacted with the electric deposit of iron and thereby allowed verification of the stimulation sites. After a minimum of 48 h, brains were cryoprotected with 25% sucrose in 0.1 M PBS until saturated and were then sectioned into 60-μm coronal sections with reference to a stereotaxic atlas (Paxinos and Watson 2007). Brain slices were then mounted onto gelatin--chromalum–coated slides and stained with cresyl violet. For verification of intracellular recording sites, cresyl violet staining was preceded by biocytin-filled neurons staining, which was achieved by using a VECTASTAIN ABC kit (Vector Laboratories, Inc., Burlingame, CA) and DAB/nickel (Sigma-Aldrich).

Results

EC Stimulation Inhibits mPFC Pyramidal Neuron Activity

Recordings were performed from a total of 129 pyramidal neurons in the prelimbic and infralimbic portion of mPFC (Fig. 1*A*). Consistent with previous studies (Floresco and Grace 2003; Laviolette et al. 2005), the baseline firing rate averaged 1 ± 0.1 Hz, whereas the percentage of spikes occurring in bursts was evaluated using previously established criteria (Laviolette et al. 2005) and calculated as 38 ± 1.8%. After recording 3 min of baseline activity, single-pulse electrical stimulation was delivered to the area of EC that has been shown anatomically to specifically project to mPFC (Insausti et al. 1997) (Fig. 1*B*). Responses were plotted using PSTHs, and 3 different responses to EC stimulation could be distinguished. Stimulation of EC induced a powerful inhibition in 110 of 129 (85.3%) neurons tested (Fig. 2*A,B,F*). In 32% (36 of 110) of those mPFC pyramidal neurons, the inhibitory response was followed by a rebound excitation (Fig. 2*B*). Most of those neurons showed inhibition at the lowest amplitude of stimulation tested (0.5 mA); however, some of the neurons that showed no/small effects at 0.5 mA stimulation were significantly inhibited at 1 mA stimulus intensity. In a different set of experiments, 22 neurons exhibited identical responses when stimulated initially at 1 mA amplitude, demonstrating that the inhibitory effects are not due to repetitive stimulation. For consistency, the onset, duration and percent of inhibition were calculated from PSTHs obtained following 1 mA stimulation of the EC (Fig. 2*A,B*; Table 1). In contrast only 10% (13 of 129) of the neurons recorded exhibited a short-latency excitation (Fig. 2*C–F*). From the observation of their latency of excitation, these neurons were divided into 2 groups. The first group consisted of all neurons that exhibited excitation with a latency ≤15 ms ($n = 6$), the second group consisted of all neurons with latencies between 16 and 50 ms ($n = 9$) (Table 1). All 13 of the neurons that showed excitation following EC stimulation continued to exhibit a potent inhibitory period (Fig. 2*C,D*). Moreover, similar to what was observed with inhibited neurons, 38.5% (5 of 13) of the excitatory response neurons exhibited a rebound excitation following the inhibitory period (data not shown). Finally, 6 of 129 neurons recorded were not responsive to EC stimulation (Fig. 2*F*). The stimulus protocol used in this study did not affect the baseline firing frequency either for the inhibitory response neurons (Kruskal–Wallis one-way ANOVA on ranks; $P > 0.05$) or the excitatory response neurons (one-way ANOVA; $P > 0.05$).

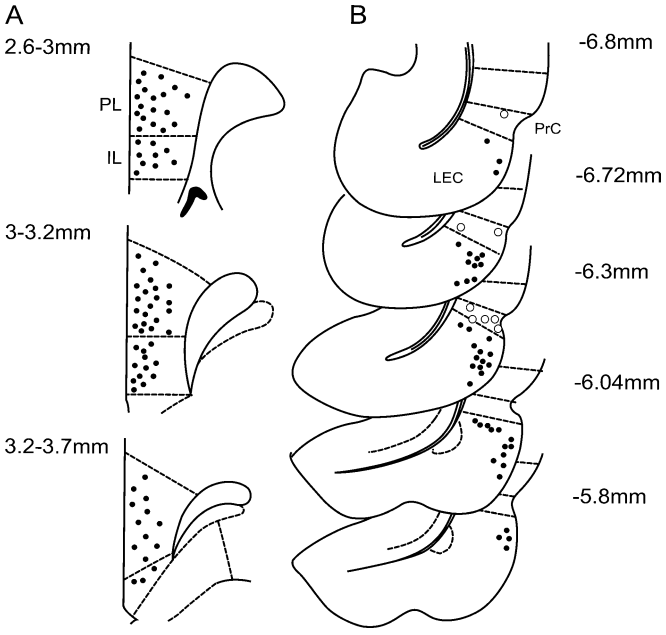

Figure 1. Histological verification of the recording and stimulation sites. For clarity, only representative, nonoverlapping samples are shown to illustrate the general anatomical distribution of the recording (*A*, prelimbic and infralimbic mPFC) and the stimulation sites (*B*, EC = filled circles; PrC = open circles).

Specificity of mPFC Neuronal Responses to the EC Stimulation

Substantial anatomical evidence suggests the existence of 2 afferent pathways of fibers from the EC to the PFC, one via the vHPC → fornix (Sesack et al. 1989; Jay and Witter 1991) and another through the PrC (Insausti et al. 1997; Delatour and Witter 2002). In order to evaluate whether the effects observed were due to stimulation of direct projections to mPFC and not to activation of long-loop collaterals, studies were performed to examine whether the observed responses were indeed due to stimulation of the EC, and not vHPC, and furthermore to examine whether the response to EC stimulation was mediated directly or via activation of the PrC.

To examine whether the vHPC was involved in the response, the vHPC (CA1 and ventral subiculum) was inactivated with 0.5 μL of 2% lidocaine (Fig. 3). All of the pyramidal neurons that were found to be inhibited by EC stimulation showed precisely the same pattern of response to EC stimulation when comparing the PSTHs obtained before (Fig. 3*A1*) versus after lidocaine application (Fig. 3*A2*), with no significant changes in the onset of response, duration, or percent inhibition after EC stimulation (paired t test > 0.05). Only 1 of 9 neurons that exhibited pure inhibition prior to lidocaine (Fig. 3*B1*) now exhibited both excitation and inhibition following EC

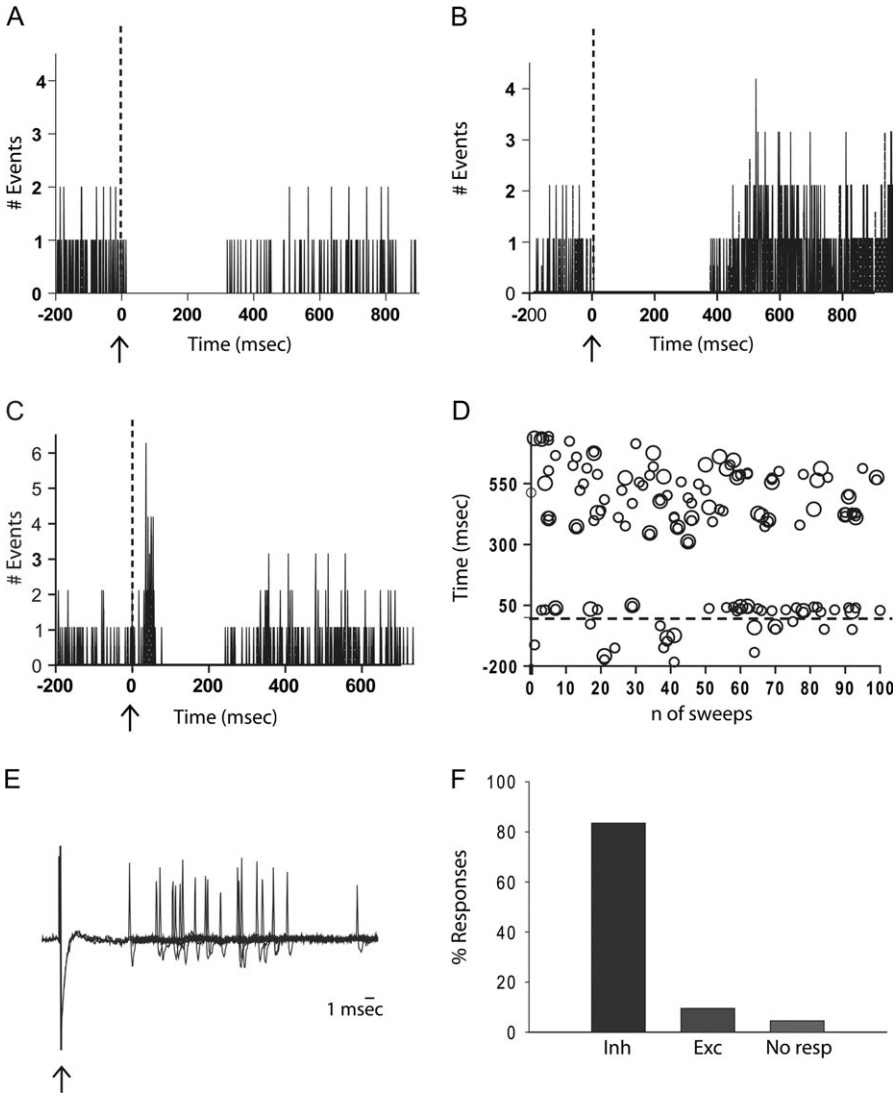

Figure 2. EC stimulation produced predominantly inhibitory responses in mPFC neurons recorded extracellularly. Peristimulus time histograms (PSTHs) illustrate responses of single mPFC neurons to single-pulse stimulation of the EC (dotted line). (*A*) PSTH of a neuron that displayed only an inhibitory response; (*B*) PSTH of a neuron that displayed inhibition and rebound excitation; (*C*) PSTH of a neuron that displayed short-latency excitation followed by inhibition; and (*D*) raster histogram of the same neuron shows responses (*y* axis) to each of the 100 stimuli (*x* axis); (*E*) an overlay of 10 consecutive evoked response traces demonstrates that the distribution of evoked spike latencies is consistent with an orthodromic monosynaptic activation (arrow indicates stimulus artifact). (*F*) Bar diagram shows distribution of response types recorded in the mPFC after stimulation of the EC. The vast majority of neurons were responsive to stimulation (96%), with 84% of the neurons exhibiting pure inhibitory responses.

Table 1
Effects of EC stimulation on mPFC pyramidal neurons

	Peak		Duration	% Effects
Single-pulse stimulation				
Inhibition $_{(PSTH)}$	17 ± 1.5 ms	—	276 ± 12.5 ms	88 ± 1.4
IPSP	49 ± 5 ms	100 ± 8 ms	317 ± 16.7 ms	—
sIPSP	20 ± 1.1 ms	27 ± 1.2 ms	—	—
Excitation$_{(PSTH)}$, Group I	6 ± 1 ms	14 ± 0.3 ms	11 ± 1 ms	212 ± 99
EPSP, Group I	11 ± 0.5 ms	26 ± 1.9 ms	—	—
Excitation$_{(PSTH)}$, Group II	9 ± 2 ms	24 ± 4 ms	22 ± 4 ms	190 ± 79
EPSP, Group II	17 ± 3 ms	27 ± 5 ms	—	—
Train stimulation				
Inhibition$_{(FR\ hist)}$	1.5 ± 0.1 s	—	28 ± 4.5 s	84 ± 4.5
Excitation$_{(FR\ hist)}$	14 ± 0.7 s	—	7 ± 2 s	191 ± 89

Note: All data are expressed as mean ± SEM. Table lists and compares data obtained both from extracellular (FR hist = firing rate histogram) and intracellular recordings following stimulation of the EC.

stimulation in a manner that was similar to the excitatory response neurons (Fig. 3*B2*). For that neuron, the onset of excitation was 25 ms, duration 13 ms, whereas the percent excitation was 63%. Overall, no significant change in baseline firing rate was observed following lidocaine application (paired *t* test, $P > 0.05$). Given that local application of lidocaine into the vHPC did not affect the EC-evoked response, it is likely that the response to EC stimulation was due to activation of direct fibers from the EC.

To confirm that responses were attributable to EC stimulation and not current spread to adjacent structures such as the PrC, the response to PrC stimulation was evaluated in 54 mPFC pyramidal neurons using the same stimulation protocol (single pulse and train) employed for stimulation of the EC. In the large majority of these neurons direct stimulation of the PrC failed to evoke any of the responses observed following EC stimulation, with essentially no change in firing rate in the PSTH obtained

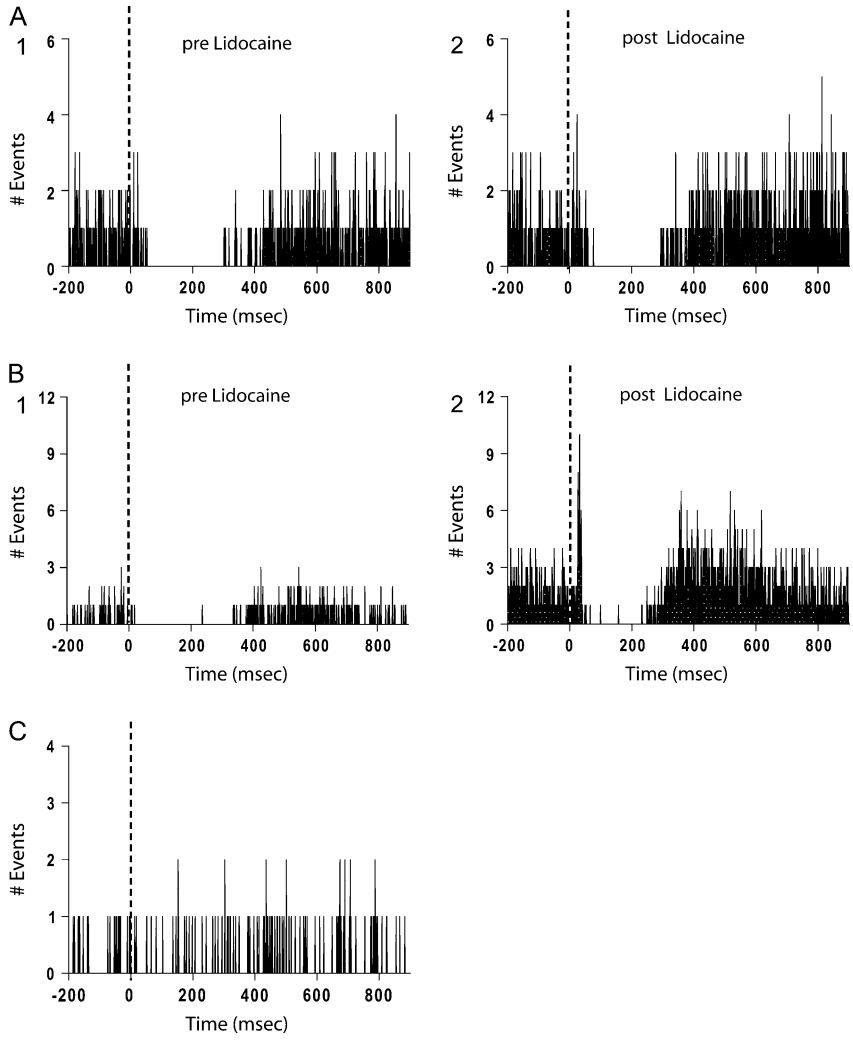

Figure 3. EC exerts its modulatory effects directly onto mPFC neurons. (*A*) PSTHs show the response of a pyramidal neuron to stimulation of the EC before (1) and after (2) lidocaine infusion into vHPC. In nearly all of the neurons recorded, inactivation of vHPC did not affect the response of mPFC pyramidal neuron to EC stimulation. (*B*) In a single case (1 out of 9 neurons tested), EC stimulation following lidocaine infusion led to the triggering of an additional excitatory response (2) compared with the pure inhibitory response of the neuron prior to lidocaine infusion (1). (*C*) PSTH of the response of a pyramidal neuron to single-pulse stimulation of the PrC. No effect of PrC stimulation was observed in the majority of the pyramidal neurons recorded extracellularly.

after stimulus (Fig. 3*C*). Only 18% of neurons exhibited an inhibitory response to PrC stimulation; however, this response was only observed when both of the following conditions were present: 1) single stimulation was delivered at higher amplitudes and 2) the stimulating electrode was located close to the border with EC (Fig. 1*B*). Thus, the effect observed may be an artifact related to current spread under the specific experimental conditions.

Taken together, these data suggest that EC stimulation potently inhibited mPFC neuron activity, and consistent with anatomical data, this inhibitory effect can be attributed to direct projections from EC to mPFC.

Evaluation of mPFC Response to Train Stimulation of EC

The effects of 20-Hz train stimulation of the EC were evaluated on a total of 32 pyramidal neurons (Fig. 4, Table 1). The neurons were first classified according to their response to single-pulse stimulation, with 25 neurons exhibiting inhibitory (Fig. 4*A1*,*B1*) and 6 neurons excitatory responses (Fig. 4*C1*), whereas one neuron was not responsive (data not shown). After train stimulation of EC, 15 of the 25 inhibitory response neurons still showed simple inhibition (Fig. 4*A2*), whereas 5 exhibited no response (data not shown). The remaining 5 pyramidal neurons exhibited a pronounced rebound excitation in addition to the inhibition, which lasted as long as 10 ms (Fig. 4*B2*). All parameters of the inhibitory responses measured from each cumulative histogram are listed on Table 1. There was no significant change in between-stimulus firing rate when compared with baseline (paired t test, $P > 0.05$).

In only 2 of 6 excitatory response neurons (Fig. 4*C1*), train stimulation evoked the same pattern of response, with excitation followed by an inhibition (data not shown). The excitation was first evident during the early course of the train stimulation. The remaining 4 excitatory response neurons displayed instead simple inhibition (Fig. 4*C2*) which appeared similar to the inhibition showed by the inhibitory response neurons (Fig. 4*A2*; Table 1).

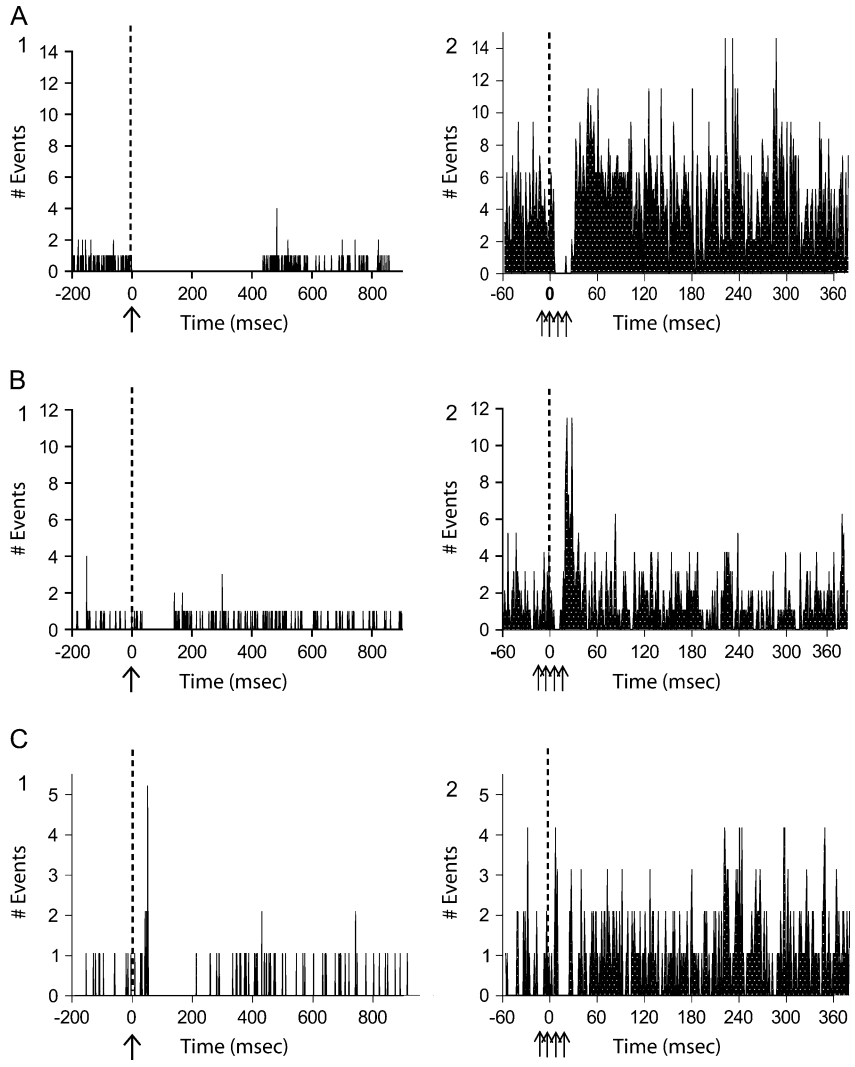

Figure 4. EC stimulation using trains of pulses evokes prolonged responses in mPFC neurons recorded extracellularly. (*A*) An mPFC neuron that exhibited single-pulse inhibition to EC stimulation (1) showed a prolonged inhibition with 20-Hz train stimulation for 5-s duration (2). (*B*) Although the majority of inhibitory response neurons displayed a similar pattern of response to trains, 5 of 25 inhibitory response neurons (1) showed a delayed and prolonged excitation following train stimulation (2). (*C*) Of the neurons that showed an initial excitation to single pulses (1), 4/6 showed only inhibition in response to train stimulation (2). For all of the above (1) is the PSTH obtained following single-pulse stimulation, (2) is the firing rate histogram following a train recorded continuously for a total of 6 min. Stimulation is indicated by dotted line.

Sharp-Electrode Intracellular Recordings from mPFC Pyramidal Neurons

The origin of the inhibitory response to EC stimulation is unknown, given that no ultrastructural studies of the connection at the synaptic level between EC and mPFC are available. Therefore, sharp-electrode intracellular recordings from mPFC pyramidal neurons were employed to assess the synaptic nature of the responses observed during extracellular recordings.

Basal activity was recorded for at least 3 min after stable impalement and, according to previous report (Yang et al. 1996; Degenetais et al. 2002), a highly heterogeneous population of neurons was observed. Thus, on the basis of their morphology, baseline activity, membrane potential histograms, and their evoked firing pattern in response to prolonged intracellular depolarizing current pulses, neurons were classified into regular spiking (RS), noninactivating intrinsic bursting (NIB), and inactivating intrinsic bursting neurons (IB; Fig. 5; Table 2). In all cases, biocytin-labeled neurons exhibited pyramidal neuron morphology, and were located in layers III–VI of the prelimbic and infralimbic regions of the mPFC, with 82% of the neurons recorded located in the superficial layers. The majority of the data on pyramidal neuron characterization have been previously examined in detail (Degenetais et al. 2002); therefore, this study focuses on describing specific characteristic that have not been extensively studied yet, such as the membrane properties and voltage oscillation.

Electrophysiological Proprieties of RS Neurons

Of the entire population of neurons recorded, 25 (50%) of the neurons were classified as RS neurons (Fig. 5*A*, Table 2). These neurons showed a sustained and regular discharge upon membrane depolarization consisting of single spikes and/or doublets (Fig. 5*A1*). In accordance with a previous study (Degenetais et al. 2002), 2 groups of RS neurons could be distinguished, namely the RS1 ($n = 10$; Fig. 5*A1*, *A2*) and RS2 ($n = 15$; Fig. 5*A1*, *A3*) neuron types. The characteristics stated above that were used to subcategorize these neurons were consistent with previous reports, and are summarized in Table 2.

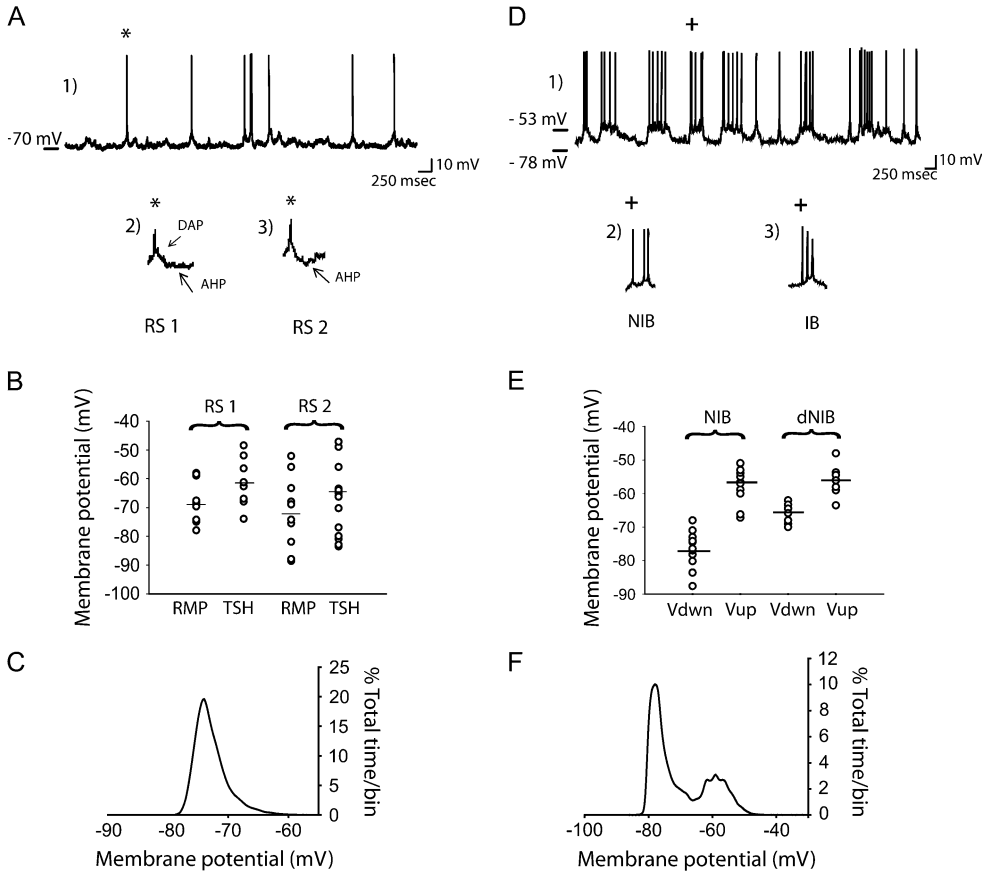

Figure 5. Membrane fluctuation properties for RS, NIB, and IB pyramidal neurons. Figure illustrates data obtained from intracellular recording and shows intrinsic membrane properties for each subtype of mPFC pyramidal neuron recorded (*A1*), Representative trace of RS neuron spontaneous activity, which consisted primarily of single action potentials; (*A2* and *A3*) magnified view of a single spike recorded from RS1 and RS2 neurons, respectively. All RS1 action potentials exhibited a fAHP (A2, arrow) and the majority also exhibited a DAP. The fAHP is particularly prominent for the RS2 action potential (A3, arrow). (*B*) Histogram of membrane potential distribution for RS1 and RS2 neurons illustrating resting membrane potential (RMP) and action potential threshold (TSH) voltage for all neurons examined. (*C*) Histogram shows membrane potential distribution over time for one single representative RS neuron. There was no evidence of a bimodal distribution of membrane potentials for all RS neurons recorded. (*D1*) Electrophysiological trace illustrating spontaneous baseline activity of a bursting neuron, consisting of down states with an absence of spike firing alternating with up states and spontaneous spike discharge. Each bistable neuron showed an all-or-none burst pattern, composed of noninactivating (*D2*, NIB) or inactivating (*D3*, IB) action potential trains. In the NIB type neurons, the bursts exhibited an increase in spike duration as the burst progressed. Furthermore, in each burst event recorded in this group of neurons, action potentials did not show a change in amplitude throughout the duration of the burst, whereas a progressive increase in spike threshold was observed across single burst events. Only IB neurons (B3) exhibited spike amplitude accommodation during burst events. (*E*) Histogram of the distribution of membrane potential for NIB neurons, showing all values of voltage for both the down and up state. Of the NIB neurons recorded, 2 different subtypes could be differentiated based on the membrane potential of the down state: NIB and dNIB. The dNIB exhibited a significantly more depolarized down state compared with the NIB neurons. (*F*) Time histogram illustrates the bimodal distribution of membrane potentials of a representative bistable neuron. Both NIB and IB neurons exhibited a biphasic membrane potential distribution.

Nevertheless, in contrast to Degenetais et al., neurons that fit the classification of RS fast-adapting neurons were not observed. Indeed, even neurons that did not exhibit spontaneous spike discharge (Table 2) demonstrated spike characteristics (Fig. *4A2*, *3*) and spike frequency adaptation following intracellular injection of depolarizing current steps that were consistent with the RS1 and RS2 classification. Moreover, there was a small difference in the percent distribution of pyramidal neuron subtypes and slightly lower average firing rate. The origin of this difference is not apparent, but may be related to electrode sampling bias or to differences in anesthetic used (sodium pentobarbital in the previous study, chloral hydrate in the current study).

Although the RS neurons tested showed some period of spontaneous membrane depolarization, this depolarization did not achieve a sustained plateau and thus none of those neurons exhibited a bistable shift in membrane potential during recording of spontaneous activity (Fig. 5*A–C*; Table 3). Instead, the membrane potential histogram obtained from those neurons exhibited a simple monophasic shape (Fig. 5*C*). Furthermore, no shift in membrane voltage occurred either following injection of intracellular current or over time.

Electrophysiological Proprieties of NIB Neurons

Of the remaining 25 mPFC neurons recorded intracellularly, 23 (46%) were classified as NIB. NIB neurons exhibited spontaneous, rapid and large-amplitude shifts in membrane potentials (Fig. 5*D1*, 2), occurring between 2 relatively stable membrane potentials separated by ~20 mV (Fig. 5*D–F*), which showed a biphasic pattern when plotted in a membrane potential histogram (Fig. 5*F*). Of all NIB pyramidal neurons recorded, a subgroup comprising 39% (9 of 23) of neurons displayed smaller fluctuations in membrane voltage; thus, this subgroup is denoted as depolarized NIB (dNIB) neurons. For all dNIB neurons fluctuations in membrane voltage resulted in significantly less of a difference between the resting membrane

potential and the plateau potential (one-way ANOVA; degree of freedom (DF) = [1, 20]; F ratio = 25.8; $P < 0.001$), and as a result the area under the plateau was smaller when compared with the more typical NIB neurons (one-way ANOVA; DF = [1, 21]; F ratio = 13.7; $P < 0.001$) (Fig. 5*E*; Table 3). Nonetheless, the smaller shift in membrane potential to the up state, which could be due at least in part to the significantly more depolarized resting membrane potential of these neurons, could clearly be differentiated from spontaneously occurring postsynaptic potentials both by the larger amplitude and the prolonged duration of these events. Furthermore, as reported previously for bistable states (O'Donnell and Grace 1995), the properties of the bistable state were not altered by depolarization or hyperpolarization of the membrane. The presence of spontaneous up states and their amplitudes is illustrated in the time histogram of the membrane potentials of individual neurons collected over periods of 20–30 s of recording (Fig. 5*F*). None of the other membrane properties were significantly different between the 2 subgroups of NIB neurons; therefore, all data were combined and are listed in Table 2.

Table 2
Electrophysiological proprieties of mPFC pyramidal neurons

	RS1 (10)	RS2 (15)	NIB (14)	dNIB (9)
Firing rate[a], silent	0.3 ± 0.1	1 ± 0.3	2 ± 0.3	See NIB
	10%	47%	18%	
% Burst	NA	NA	60 ± 5.8	See NIB
RMP/V_{down}[b]	–68 ± 2.9	–74 ± 3.2	–77 ± 1.5*	–66 ± 1.2*
$V_{threshold}/V_{up\ stat}$[b]	–61 ± 2.9	–68 ± 3.2	–57 ± 1.3	–56 ± 1.8
Coefficient of variation[c]	0.3 ± 0.02	0.4 ± 0.02	NA	NA
AP_{ampl}[b]	65 ± 2.4	60 ± 2.2	62 ± 1.7	See NIB
$AP_{1/2width}$[d]	0.9 ± 0.08	1 ± 0.1	1 ± 0.1	See NIB
τ[d]	11 ± 2.4	10 ± 1.4	9 ± 0.8	See NIB
R_i[e]	40 ± 1.6	42 ± 3 MΩ	41 ± 2.6 MΩ	See NIB
Rectification	25%	40%	28%	
No-rectification	75%	60%	72%	See NIB

Note: All data are expressed as mean ± SEM. *Statistically different: V_{down} of NIB versus V_{down} of dNIB. One-way ANOVA; DF = [1,20], F ratio = 26.5, $P < 0.01$
[a]Firing rate is measured in Hz.
[b]Resting membrane potential (RS neurons), membrane voltage of down state (NIB neurons), membrane voltage at threshold (RS) or membrane voltage of up state (NIB) as well as action potential amplitude are all measured in mV.
[c]Coefficient of variation of membrane voltage, measured as SEM/mean of RMP.
[d]Action potential amplitude calculated at half width and membrane time constant (τ) calculated at 63% plateau are expressed in ms.
[e]Input resistance (R_i) expressed in MΩ.

Electrophysiological Properties of IB Neurons

Only 2 of the neurons encountered were classified as intrinsic bursting (IB). IB neurons show numerous similarities with NIB, such as a comparable pattern of discharge (Fig. 5*D1*), mean spontaneous firing frequency, and mean firing rate within a burst. However, each burst of IB pyramidal neurons displayed a progressive decrease in action potential amplitude (Fig. 5*D3*), which fit the characteristics described previously for "inactivating-bursting" neurons (Baranyi et al. 1993; Degenetais et al. 2002).

Single-Pulse Stimulation of the EC Evokes Excitatory/Inhibitory Events

The response of mPFC pyramidal neurons, classified according to the aforementioned criteria, to single-pulse stimulation of the EC was evaluated. Single-pulse electrical stimulation delivered to the lateral EC induced a complex synaptic response in mPFC pyramidal neurons (Fig. 6*A*), which exhibited similar properties as that described for all 3 electrophysiological classes of neurons examined. For simplicity, the evoked postsynaptic events in 36 pyramidal neurons recorded intracellularly are reported. In the majority of neurons tested, this response consisted of an early EPSP (Fig. 6*A*,*B*), with single or multiple IPSP components (Fig. 6*A*). Furthermore, in 50% of RS1 neurons tested the early EPSP was followed by a late-occurring EPSP (Fig. 6*C*). Two of the 36 neurons (1 RS2 and 1 NIB) did not exhibit any postsynaptic events following EC stimulation.

Excitatory Postsynaptic Potentials

EC stimulation induced early EPSPs in 28 out of 36 (78%; 14 RS and 14 NIB) of the pyramidal neurons examined (Fig. 6*B*), and similar to what was observed in single-unit recording, these events could be differentiated into 2 groups (Table 1). In every case, the responses exhibited an increase in amplitude and constant onset latencies with increasing stimulus intensities, which is consistent with a monosynaptic event. The amplitude of the excitatory component was dependent on 2 factors: 1) the baseline membrane potential, and 2) the type of

Table 3
Effects of EC stimulation on RS2 and NIB pyramidal neurons

	$V_{up} - V_{dwn}$	Area	Duration	% Time	# Events/min	Frequency
RS2 baseline	6 ± 0.5	1702 ± 204.6	459 ± 47.5	33 ± 5.8	43.5 ± 6.9	0.7 ± 0.1
0.1 mA	8.3 ± 1.5	3352 ± 557.6*	843.3 ± 106*	44.8 ± 8.4	31.7 ± 5.3	0.5 ± 0.09
0.5 mA	9 ± 1.3*	3486 ± 330.7*	817 ± 67.6*	49.8 ± 7.4	39.2 ± 6.8	0.6 ± 0.1
1 mA	11 ± 1.5*	6917 ± 1610.3*	1568 ± 352.4*	69 ± 1.9*	34.4 ± 8.4	0.6 ± 0.1
dNIB baseline	10 ± 1$^+$	3393 ± 514.5$^+$	653 ± 71.9	53 ± 3	55 ± 3.5	0.9 ± 0.06
1 mA	10.5 ± 1.6	7049 ± 2132.7**	1389 ± 437.3**	64 ± 2.5**	36 ±6.5**	0.6 ± 0.1**
NIB baseline	20 ± 1.4$^+$	6412.3 ± 562.7$^+$	768.8 ± 38.3	65.1 ± 2.8	48.5 ± 1.5	0.8 ± 0.01
1 mA	19.4 ± 1.8	7691.1 ± 1499.1	1006.3 ± 111.6	66 ± 4.5	46.8 ± 3	0.8 ± 0.05

Note: *Statistically different from baseline. Baseline versus 0.1 mA stimulus: Area (one-way ANOVA; DF = [1, 16], F ratio = 11.7, $P = 0.03$); duration (one-way ANOVA; DF = [1, 16], F ratio = 14.9, $P = 0.01$). Baseline versus 0.5 mA stimulus: $V_{up} - V_{dwn}$ (Kruskal–Wallis one-way ANOVA on Ranks test; diff. of ranks = 5.6, $Q = 2.2$, $P < 0.05$); area (DF = [1, 18]; F ratio = 23.6; $P < 0.001$); duration (one-way ANOVA; DF = [1, 18]; F ratio = 20; $P < 0.001$). Baseline versus 1 mA stimulus: $V_{up} - V_{dwn}$ (one-way ANOVA; DF = [1, 14], F ratio = 14.7, $P = 0.02$); Area (Kruskal–Wallis one-way ANOVA on Ranks test; diff. of ranks = 8.5, $Q = 3.2$, $P < 0.05$); duration (Kruskal–Wallis one-way ANOVA on Ranks test; diff. of ranks = 7.9, $Q = 2.9$, $P < 0.05$); % time (Kruskal–Wallis one-way ANOVA on Ranks test; diff. of ranks = 7.6, $Q = 2.8$, $P < 0.05$).
**Statistically different from baseline. Baseline versus 1 mA stimulus: Area (DF = [1, 11]; F ratio = 5.5; $P < 0.05$); Duration (Fig. 8*B*,*C*) (DF = [1, 10]; F ratio = 5.6; $P < 0.05$); % Time (DF = [1, 11]; F ratio = 5.2; $P < 0.05$); # Events/min (DF = [1, 11]; F ratio = 7.7; $P < 0.05$); Frequency (DF = [1, 11]; F ratio = 7.7; $P < 0.05$).
$^+$Statistically different: baseline of dNIB versus baseline of NIB. $V_{up} - V_{dwn}$ (one-way ANOVA; DF = [1, 20]; F ratio = 25.8; $P < 0.001$); Area (one-way ANOVA; DF = [1, 21]; F ratio = 13.7; $P = 0.001$). None of the parameters of the NIB neurons were significantly altered by EC stimulation (pre versus poststimulus, one-way ANOVA; $P > 0.05$).
In all PSTHs, the dotted line indicates delivery of the stimulus pulse.

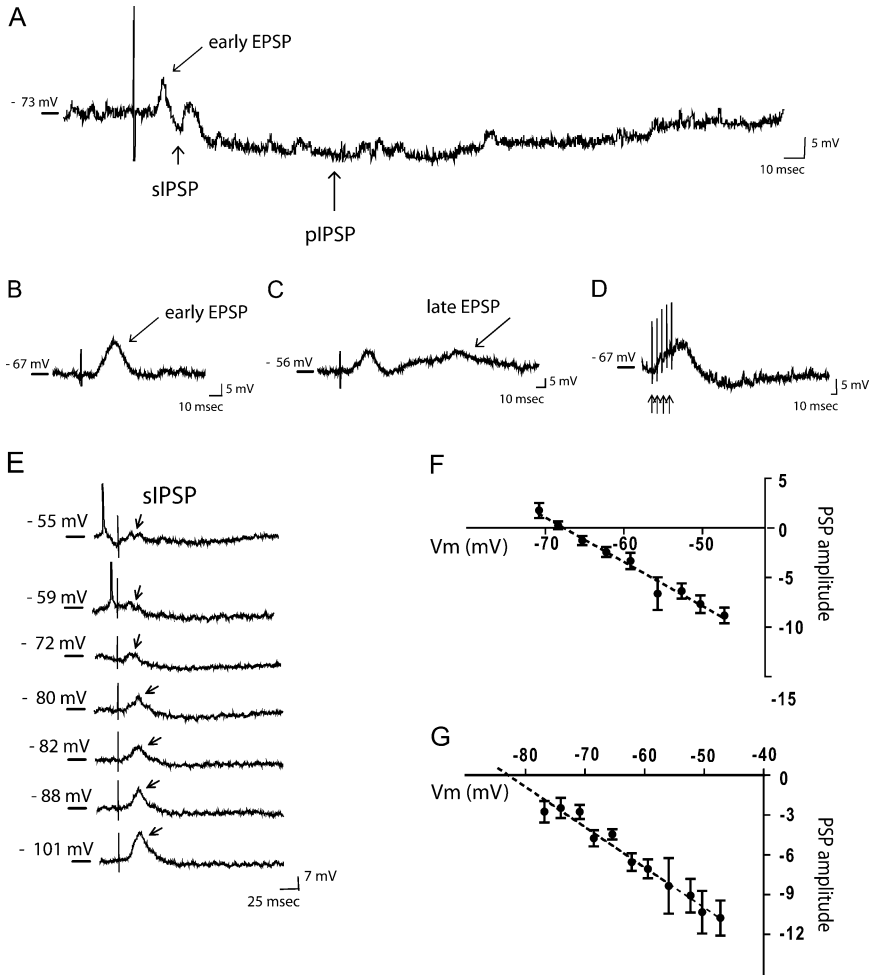

Figure 6. Stimulation of EC evokes both excitatory and inhibitory postsynaptic responses in mPFC neurons. (*A*) Representative trace from a RS pyramidal neuron shows a mix of postsynaptic responses evoked following EC stimulation; in particular, the trace illustrates the presence of both a short, fast IPSP (sIPSP, arrow) and a pIPSP (arrow), subsequent to the elicitation of an early EPSP. (*B*) Trace shows a detail of an early EPSP (arrow), followed by an inhibitory response. (*C*) In this neuron, single-pulse stimulation of the EC evokes an early EPSP and late EPSP (arrow). (*D*) Example traces of train stimulation that evokes a more pronounced EPSP. (*E–G*) The sIPSP and the pIPSP exhibited distinct reversal potentials. (*E*) Depolarizing or hyperpolarizing the membrane of this neuron from resting membrane potential (−69mV; arrow) shows a reversal of the sIPSP component (arrows) at ~ 69 mV. Each trace was obtained by injecting 0.2 nA steps of current. (*F*) Plotting the amplitude of the short-latency IPSP against the membrane potential at which it was evoked demonstrates a reversal potential of −69.5 mV in this case, which is consistent with activation of a Cl^- conductance. (*G*) Plotting the amplitude of the pIPSP versus membrane potential reveals a reversal potential of −83 mV in this case, which is consistent with activation of K^+ conductances. PSP amplitude= postsynaptic potential amplitude. In all traces, the vertical line represents the stimulus artifact.

stimulation, with train stimuli inducing a larger depolarizing response (Fig. 6*D*). As EPSPs always were evoked in association with an IPSP, which usually overlapped temporally with the EPSP, it was not possible to accurately estimate the EPSP amplitude and duration (Fig. 6*A*).

The evoked EPSP triggered spike discharge in 6 of the neurons tested (3 RS and 3 NIB neurons). The late EPSP displayed an average latency of 143 ± 14.6 ms, and always followed the early EPSP component (Fig. 6*C*). In each case where a late EPSP occurred, the neuron was classified as the RS type 1.

Inhibitory Postsynaptic Potentials

The IPSP that typically followed an early EPSP was small, averaging 8 ± 1.4 mV in amplitude at resting membrane potential (Table 1). Upon membrane hyperpolarization, the IPSPs could be differentiated into an early and a late component (Fig. 6*A*; Table 1) and increasing the intensity of EC stimulation resulted in a larger amplitude and longer duration inhibitory components. Furthermore, the onset latency of the early IPSPs and the duration of the late IPSP were consistent with the latency and duration of the inhibition observed during extracellular recording (Table 1). As a consequence of the inhibition, all responsive neurons showed a complete cessation of firing for the duration of the late IPSP. The nature of the evoked IPSPs was examined by testing the effects of membrane hyperpolarization and depolarization on the evoked potential amplitude (Fig. 6*E–G*). The mean reversal potential of the early IPSP was –70 ± 1.6 mV (Fig. 6*F*), whereas the mean reversal potential of the pIPSP was –80 ± 3.3 mV (Fig. 6*G*). Taken together, these data are consistent with previous studies performed in vitro in neocortical slices (Connors et al. 1982; Howe et al. 1987) and during in vivo intracellular recording (Szente et al. 1988; Agmon and Connors 1992; Baranyi et al. 1993; Nunez et al. 1993; Branchereau et al. 1996; Degenetais et al. 2003) indicating that evoked inhibitory responses were composed of an early $GABA_A$-mediated IPSP and a late $GABA_B$-mediated IPSP. The more negative reversal potential of the late IPSP may be indicative of a distal site of generation, and is

consistent with the reversal potential reported by others for this late, putative $GABA_B$-mediated event (i.e., –78 mV).

Excitatory Effects of EC Stimulation on dNIB and RS2 Neuron Activity

The effects of EC stimulation on membrane voltage and firing activity was examined in each of the subtypes of mPFC pyramidal neurons recorded. All responses were studied using several stimulus intensities. EC stimulation resulted in a direct depolarization of membrane potential in RS2 (Fig. 7) and dNIB (Fig. 8) neurons. Even though EC stimulation evokes postsynaptic responses in all RS1 and NIB neurons (indicating that these neurons also receive fibers from the EC), none of those neurons exhibited changes in membrane potentials.

Effect of EC Stimulation on RS2 Neuron Activity

The effects of EC stimulation were examined in a total of 15 RS2 neurons. All amplitudes of single-pulse current stimulation of the EC tested caused a pronounced depolarization of the membrane potential, with the effects increasing with increasing amplitudes of stimulation current (one-way ANOVA; Fig. 7 and Table 3). Repeated train stimulation was also evaluated in few neurons of each type; in all cases the results were similar to those observed following single-pulse stimulation, with the only difference being a more pronounced increase in amplitude and duration of the EPSP and in particular of the IPSP (Fig. 7*C*).

At 0.5 mA of EC stimulation, a significant and robust increase in the up state duration (Fig. 7*B,D*) (DF = [1, 18]; F ratio = 20; $P < 0.001$) and of the area under the curve (i.e., difference between up state potential and RMP × time) (Fig. 7*B,E*) (DF = [1, 18]; F ratio = 23.6; $P < 0.001$) was observed. Furthermore, there was a significant difference in membrane voltage between the resting membrane potential and spike threshold voltage, which is identified as the "amplitude of depolarization" in Figure 7 (Kruskal–Wallis one-way ANOVA on Ranks test; diff. of rank = 5.6; $Q = 2.2$; $P < 0.05$; Fig. 7*B,F*; Table 3). No difference in the percent of time that the neuron membrane potential spent in a more depolarized state was observed when baseline values were compared with values obtained following 0.5 mA stimulation (one-way ANOVA; $P > 0.05$). Nevertheless, a significant increase was observed following single-pulse stimulation at 1 mA when compared with baseline (Kruskal–Wallis one-way ANOVA on Ranks test; diff. of rank = 7.6; $Q = 2.8$; $P < 0.05$) (Fig. 7*G*; Table 3). Furthermore, single-pulse stimulation of the EC at 1 mA induced a significantly larger increase in the area under the curve when compared with the effects obtained at 0.5 mA (Kruskal–Wallis one-way ANOVA on Ranks test; diff. of rank = 4.9; $Q = 2.2$; $P < 0.05$). However, no significant difference in duration or amplitude of depolarization was observed when comparing the effects of lower current intensities (0.1 and 0.5 mA) with 1 mA (Kruskal–Wallis one-way ANOVA on Ranks test or one-way ANOVA; $P > 0.05$). Moreover, none of the amplitudes of EC current stimulation tested produced a significant effect on the number of depolarized states when compared with baseline (data not shown). The latency of the induced shift in membrane potential averaged 356 ± 50 ms following 0.5 mA stimulation of EC, whereas at 1 mA the latency was 582 ± 148 ms. The majority of RS2 pyramidal neurons examined exhibited this direct excitatory effect. Although the evoked EPSP was typically found in association with an evoked depolarization of the membrane potential, 3 of the 15 RS2 pyramidal cells that exhibited EPSPs in response to EC stimulation did not show any depolarization of the membrane potential. Progressive depolarization or hyperpolarization of the membrane of 7 of the 12 neurons recorded was effective in altering spike firing frequency; however, it did not alter the frequency of occurrence or amplitude of the up state events. This finding is consistent with previous reports of bistable neuron properties in the nucleus accumbens (O'Donnell and Grace 1995).

Effect of EC Stimulation on NIB Neuron Activity

Overall, single-pulse stimulation did not produce a significant response in the population of NIB neurons tested ($n = 23$). Nonetheless, if the population is divided into NIB and dNIB neurons, single-pulse stimulation of EC induced a direct excitation only in the depolarized subset of NIB neurons ($n = 9$; Fig. 8). The response was observed only with the highest stimulation amplitudes of 1 mA, with no significant responses at lower current intensities of 0.1 and 0.5 mA (one-way ANOVA; $P > 0.05$). Furthermore, as above, there were no differences (other than magnitude of response) in the type of effects produced by train versus single-pulse stimulation (Fig. 8*C*).

Thus, stimulation of EC at 1 mA affected the depolarized plateau state, with an increase in the duration (Fig. 8*B,D*) (one-way ANOVA; DF = [1, 10]; F ratio = 5.6; $P = 0.04$), in the area under the curve of the plateau depolarization (Fig. 8*B,E*) (one-way ANOVA; DF = [1, 11]; F ratio = 5.5; $P = 0.04$), and in the percentage of time that each neuron spent in the up state (Fig. 8*B,F*; Table 3) (one-way ANOVA; DF = [1, 11]; F ratio = 5.2; $P = 0.04$). However, stimulation of EC induced a significant decrease of the number of up states (Fig. 8*B,G*) (one-way ANOVA; DF = [1, 11]; F ratio = 7.7; $P = 0.02$), and consequently in the frequency of up states (Fig. 8*B,H*; Table 3) (one-way ANOVA; DF = [1, 11]; F ratio = 7.7; $P = 0.02$), potentially as a result of the increase in duration of the events. Stimulation of the EC did not result in any significant changes in the membrane voltage difference between up and down states of dNIB or in firing rate or in resting membrane potential (one-way ANOVA; $P > 0.05$). It is worth noting that following EC stimulation both the area under the curve and the duration of up states of dNIB were not significantly different when compared with area and duration of up states in NIB neurons (one-way ANOVA; $P > 0.05$) (Fig. 8*D,E*).

Discussion

This study represents the first investigation of EC modulation of mPFC pyramidal neuron activity. The primary finding of this study is that the vast majority of mPFC recorded neurons were exclusively inhibited following EC stimulation, and of those few neurons that were excited, a prolonged inhibition was observed to follow the short-latency excitation. Furthermore, the intracellular study confirmed that the inhibition observed was sustained and prolonged likely due to the activation of both $GABA_A$ and $GABA_B$ receptors. Both stimulation of PrC or inactivation of the HPC–mPFC pathway failed to alter the mPFC response to EC, suggesting that EC is modulating mPFC neurons activity through the direct EC–mPFC pathway. In addition, this study provides the first evidence that, in specific subpopulations of mPFC pyramidal neurons, up states can be modulated by afferents from a region external to neocortical intrinsic loops, as stimulation of the EC induced a significant

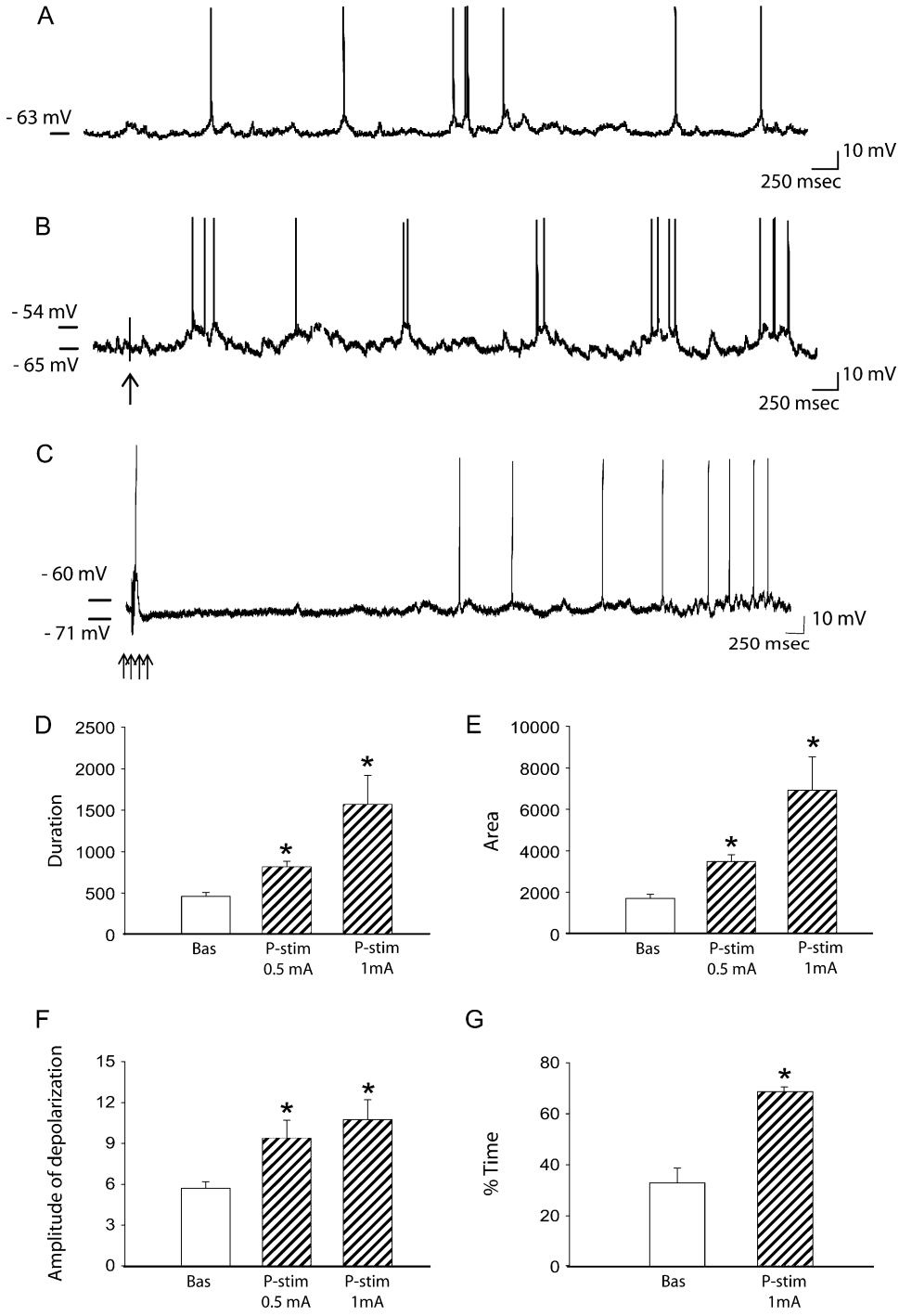

Figure 7. EC stimulation increases up state activity in RS2 pyramidal neurons. (*A*) Baseline activity of an RS2 neuron. (*B*) Following 0.5 mA single-pulse stimulation of the EC (arrow indicates stimulus artifact), this same neuron now exhibits enhanced spiking and up state activity. (*C*) Train stimulation evoked pronounced IPSPs which lead to a delayed increase on membrane depolarization. (*D–G*) Increasing amplitudes of single-pulse EC stimulation (0.5 and 1.0 mA) caused increased activation of up states in RS2 neurons, as demonstrated by the increase in (*D*), up state duration, (*E*), area above Vm, and (*F*), amplitude of the up state. Furthermore, EC stimulation induced an increase in (*G*), the percentage of time spent in a more depolarized state, but only when 1 mA stimulation was used. Bas = baseline; P-stim = poststimulation, at the 2 current amplitudes (0.5 and 1 mA, respectively) tested (*one-way ANOVA; $P < 0.05$; $^{+}$ and $^{\#}$Kruskal–Wallis one-way ANOVA on rank; $P < 0.05$).

increase in the depolarized states in 2 subtypes of mPFC pyramidal neurons recorded intracellularly.

EC Activation Potently Inhibits mPFC Neuron Activity

Numerous anatomical studies have revealed a widespread projection from EC to mPFC (Sarter and Markowitsch 1985; Swanson and Kohler 1986; Insausti R et al. 1997), which would suggest an extensive innervation of PFC. In accordance with those studies, our data show that the vast majority of mPFC neurons recorded both in the prelimbic and infralimbic mPFC responded to EC stimulation, with the predominant effect being inhibition. Moreover, using intracellular recordings, we

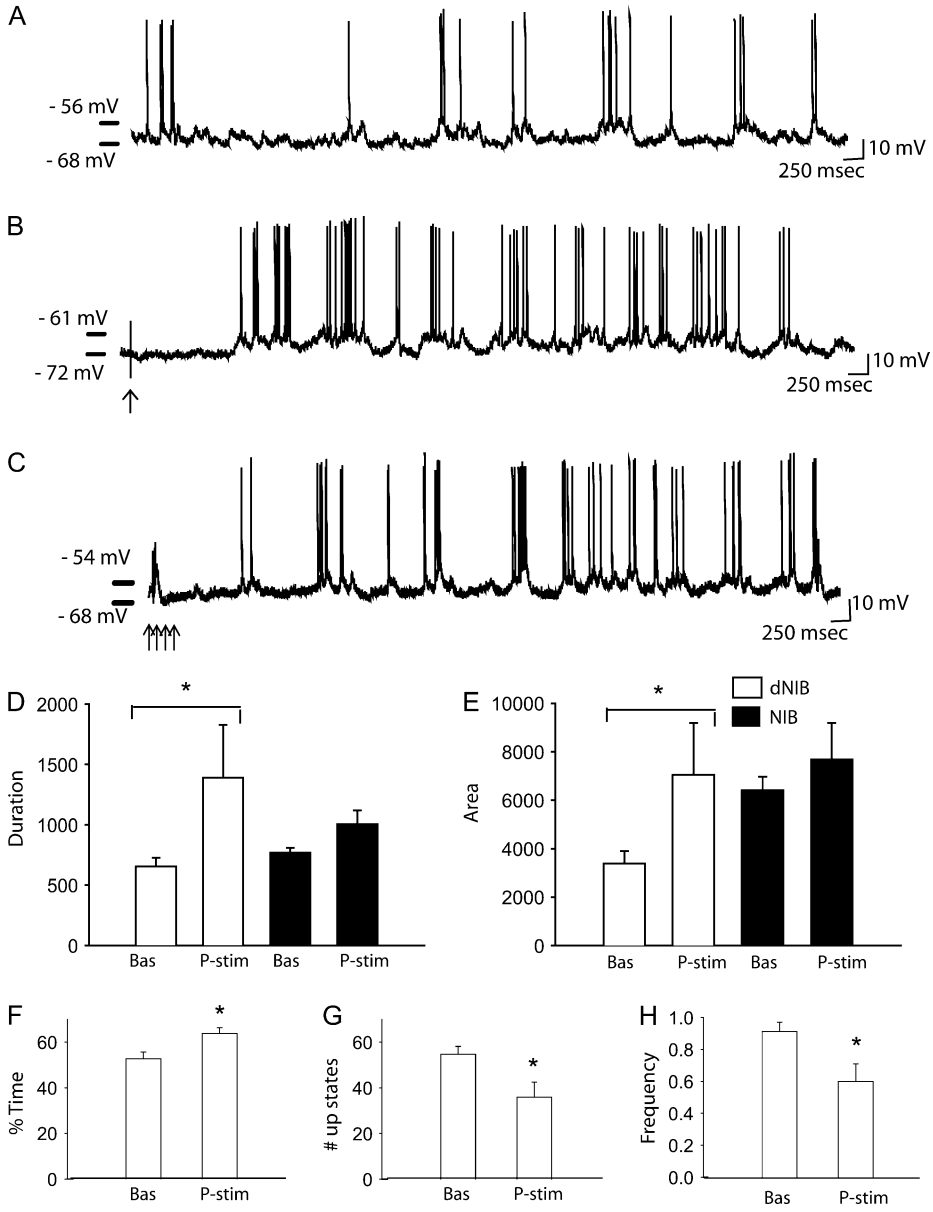

Figure 8. EC stimulation increases up state activity selectively in dNIB but not NIB mPFC pyramidal neuron subtypes. (*A*) Baseline activity of a dNIB neuron with a resting membrane potential (Vm) −68 mV. (*B*) Following 1 mA single-pulse EC stimulation (arrow indicates stimulus artifact), this same neuron now exhibits enhanced up state activity. (*C*) Details of the effects of train stimulation on membrane depolarization. Across all NIB neurons tested, single-pulse stimulation of the EC caused an increase in the up states only in the dNIB neurons in terms of up state duration (*D*) and area above Vm (*E*); the increase in up state duration was coupled with an increase in the percent time in the up states (*F*). However, EC stimulation caused a decrease in the number of up states (*G*) and frequency of up state occurrence (*H*). None of these parameters were altered in the NIB type neurons. Bas = baseline; P-stim = poststimulation (*one-way ANOVA; $P < 0.05$).

found that in virtually all pyramidal neurons examined stimulation of EC induced multiphasic synaptic responses consisting of a pIPSP usually accompanied by an early EPSP and/or short-duration IPSP.

In many cases, epochs of stimuli can exert substantially different effects than observed with single-pulse stimuli, due to the recruitment of interneurons or recruitment of long-loop afferents. In our experience (Rosenkranz et al. 2003; Onn and Wang 2005), a train of stimuli may be more reflective of the response of the system to tonic activation of an afferent. For this reason, the effect of 20-Hz train stimulation of the EC was tested. However, data obtained from both extracellular and intracellular recordings indicate that train stimulation produced qualitatively similar but quantitatively larger inhibition, both in terms of percent of responses and duration, when compared with the responses evoked by single-pulse stimulation of the EC.

Because of the number of projections between the hippocampal formation and the mPFC, it is necessary to evaluate whether the effects observed are derived exclusively from the area stimulated. Previous anatomical studies (Jay and Witter 1991; Delatour and Witter 2002) have shown that the EC exhibits a substantial projection to the vHPC; thus, EC stimulation could also drive an indirect EC → vHPC → mPFC pathway. Nonetheless, the observation that inactivation of the vHPC with lidocaine failed to affect the response strongly

suggests that the modulatory effects observed in this study were mediated directly by EC afferents to the mPFC. Furthermore, given that train stimulation of the EC-evoked responses similar to those evoked by single stimuli, it is likely that the response was not polysynaptic in nature. Moreover, the PrC is anatomically contiguous to the EC and evidence shows that the PrC provides a dense innervation of frontal cortical regions (Insausti et al. 1997). However, PrC stimulation did not mimic the effects of EC stimulation, thus ruling out current spread to this structure in the responses obtained.

These results are consistent with other recent reports showing that excitatory afferents to the mPFC arising from a variety of regions, including the amygdala (Ishikawa and Nakamura 2003; Floresco and Tse 2007) and HPC (Degenetais et al. 2003), produce potent inhibition of activity within the mPFC. Furthermore, our findings are consistent with previous reports where activation of afferent cortical pathways in vivo (Szente et al. 1988; Agmon and Connors 1992; Baranyi et al. 1993) as well as local stimulation in vitro (Howe et al. 1987; Sutor and Hablitz 1989; Chagnac-Amitai et al. 1990; de la Pena and Geijo-Barrientos 1996) evoked an EPSP followed by a long-lasting inhibition, which consisted of a fast Cl^--mediated $GABA_A$ response and a slow K^+-mediated $GABA_B$ response (Kelly and Krnjevic 1969; Avoli 1986; Connors et al. 1988; Karlsson et al. 1988; Deisz and Prince 1989). In addition, IPSPs evoked from HPC have been shown, using specific antagonists, to consist of both a $GABA_A$ and a $GABA_B$ inhibitory component (Degenetais et al. 2003; Tierney et al. 2004). Alternately, there is evidence that metabotropic glutamate receptor-mediated Ca^{2+} waves could also affect mPFC pyramidal neuron excitability by activating small conductance calcium activated potassium channels, which would evoke a transient hyperpolarization followed by a sustained depolarization (Hagenston et al. 2008). In an ultrastructural study, CA1 hippocampal afferents to the mPFC were shown to innervate parvalbumin-containing neurons as well as pyramidal neurons (Gabbott et al. 2002). If a similar anatomical configuration is present with respect to EC innervation of the mPFC, it is likely that the inhibitory effects observed in our extracellular recordings were due to direct activation of interneurons which in turn would inhibit pyramidal neurons. Of course, in the absence of ultrastructural studies addressing EC–mPFC afferents, it cannot be determined conclusively whether EC stimulation elicits IPSPs via activation of local interneurons, activation of recurrent collaterals, or a combination of actions. In any event, activation of an inhibitory local collateral system would serve to temporally limit the efficacy of excitatory inputs arising from the EC.

Direct Excitatory Effect of EC Stimulation on RS2 and NIB Neurons

Of the entire population of neurons recorded, ~10% exhibited a short-latency, orthodromic excitation, which in all cases preceded the inhibition. In terms of onset and latency of the peaks, the excitation observed extracellularly was temporally correlated with the early EPSPs evoked during intracellular recordings. The early EPSP amplitude was membrane voltage-dependent, and exhibited a short, constant onset latency, similar to that reported by others for hippocampal inputs (Degenetais et al. 2003). Previous in vitro studies (Hablitz and Sutor 1990) indicate that early EPSPs are mediated by activation of AMPA receptors, which is consistent with the observed modulation of EPSP amplitude by membrane polarization. Half of the RS1 neurons recorded also exhibited a late EPSP, which was separated from the initial EPSP by an intervening IPSP. Whether the late EPSP originated from local circuits or long-loop afferents is not well understood. Previous in vitro studies (Komatsu et al. 1991; D'Antuono et al. 2006) have shown that late EPSPs can be evoked in brain slices, suggesting that they may arise from local circuit connections; however, this explanation does not role out participation of a long-loop circuit in the generation of the late EPSP.

Stimulation of the EC significantly affected the activity state of the dNIB and nearly all RS2, but not RS1 neurons. Both on RS2 and in dNIB neurons, EC stimulation induced a significant enhancement of up states with an overall prolongation of the depolarized state. The NIB were segregated into 2 groups, the NIB and the dNIB, primarily on the basis of the observation that dNIB neurons exhibited a more depolarized RMP, and therefore smaller amplitude up state transitions. However, given the data showing a differential effect of EC stimulation on up states only in the dNIB neurons, it is likely that the segregation may relate to more than just resting membrane state, but may be indicative of differential innervation or intrinsic excitability. This will require further studies for clarification. A similar scenario is conceivable with respect to the RS1 and RS2 neurons, with the selective excitatory effect observed with RS2 neurons originating either from differential innervation or intrinsic membrane properties. The finding that a pronounced and sustained up state can be induced by EC stimulation on a subtype of neuron which typically would not display such a characteristic (i.e., the RS type 2 neurons), is of particular interest given the role of mPFC and EC in many physiological as well as pathological conditions. Even though the values of area of the depolarizing plateau, number of up states and percentage of time spent in up states of RS2 neurons following EC stimulation were similar to those of the NIB neurons, the RS2 pyramidal neurons did not display any significant alterations in either burst activity or in firing rate. Nevertheless, at all current intensities tested, stimulation of the EC did not induce substantial changes in membrane voltage, in the coefficient of variation or in the up state amplitude histogram, which even after EC stimulation showed no change from the monophasic membrane potential distribution typical of the RS neurons to the biphasic distribution characteristic of bursting neurons. This suggests that in the RS2 pyramidal neuron class, although the depolarization induced by EC was prominent and sustained, it did not evoke a state consistent with the defined bistable state as observed in the NIB or IB neurons and may support the evidence that the bistable state depends in part on intrinsic membrane proprieties of these 2 subclasses of neurons. Thus, the data presented in this study suggest that the excitatory effect on dNIB and RS2 are mediated via synaptic inputs, because direct membrane polarization failed to influence the up states of these neurons. In contrast, stimulation of other afferent projections to the PFC, including the HPC, has not been reported to affect the bistable state of mPFC neurons (Degenetais et al. 2003).

Significance of the Up and Down States in Brain Functioning

In accordance with numerous researchers (Steriade et al. 1993a, 1993b; Cossart et al. 2003), recordings from NIB and IB neurons revealed the presence of a clear and sustained slow oscillation in membrane potential, characterized as the bistable

up and down states. There is substantial evidence indicating that neurons in the neocortex display slow rhythmic activity during anesthesia and slow wave sleep (Steriade et al. 1993; Cowan and Wilson 1994; Timofeev et al. 2001; Petersen et al. 2003). This activity is believed to arise from several factors, including reverberation within local neuronal networks (Steriade et al. 1993; McCormick et al. 2003), and intrinsic pyramidal neuron membrane properties (Amzica and Steriade 1995; Wilson and Kawaguchi 1996; Gabel and Nisenbaum 1998; Sanchez-Vives and McCormick 2000; Cunningham et al. 2006). Thus, vHPC lesions disrupt up states (O'Donnell et al. 2002), and in the current study, we found that the EC can potently regulate up–down transitions within the mPFC. Whether the bistable states are present in awake animals is still under investigation; however, recent data show that long-duration event-related up states, as determined by calcium imaging and recordings (Crochet et al. 2005; Kerr et al. 2005), have suggested that these events are present and may gate information flow during normal behavior.

Several hypotheses have been elaborated to explain the functional significance of up and down states. Bistable states have been proposed to underlie functional gating of information flow (O'Donnell and Grace 1995) and synchronized membrane fluctuations have been proposed to represent the means by which the nervous system stores bit of information (Fusi et al. 2005). Thus, a combination of synaptic, dendritic, neuronal and network activity that drive bistable states could provide a powerful influence over neuronal processing and encoding of input. A recent study indicates that cortical slow oscillations drive neurons of the PFC, somatosensory, entorhinal, and subicular cortices into synchronous transitions between up and down states. Furthermore, coordinated alternation of activity and silence extends from the PFC to many regions of the hippocampal formation via the EC, allowing a reset and temporal harmonization of the neo/paleocortical and hippocampal network (Isomura et al. 2006). Therefore, drawing from the current and previous studies, the PFC → EC → HPC system appears to constitute a self-organizing and temporally coordinated loop through which several mnemonic and intellectual processes may be synchronized. The ability of the EC to regulate mPFC bistable states may provide a means to achieve such regulation. Thus, by gating information flow via regulation of up states, the EC would be in a position to gate mPFC output based on experience-determined constraints. Plasticity within this circuit in the form of LTP and LTD (Floresco and Grace 2003; Goto and Grace 2006; Kawashima et al. 2006) could refine the degree to which the EC may exert such control based on prior learning experiences.

Funding

United States Public Health Service National Institute of Mental Health Grant (MH45156)(AAG).

Notes

We would like to thank Nicole MacMurdo and Christy Smolak for their technical support and Brian Lowry for production, development, and assistance with the custom-designed electrophysiology software (Neuroscope). *Conflict of Interest*: None declared.

Address correspondence to Ornella Valenti, Department of Neuroscience, University of Pittsburgh, A210 Langley Hall, Pittsburgh, PA 15260, USA. Email: valenti@pitt.edu.

References

Agmon A, Connors BW. 1992. Correlation between intrinsic firing patterns and thalamocortical synaptic responses of neurons in mouse barrel cortex. J Neurosci. 12:319–329.

Amzica F, Steriade M. 1995. Short- and long-range neuronal synchronization of the slow (< 1 Hz) cortical oscillation. J Neurophysiol. 73:20–38.

Amzica F, Steriade M. 1998. Electrophysiological correlates of sleep delta waves. Electroencephalogr Clin Neurophysiol. 107:69–83.

Avoli M. 1986. Inhibitory potentials in neurons of the deep layers of the in vitro neocortical slice. Brain Res. 370:165–170.

Baranyi A, Szente MB, Woody CD. 1993. Electrophysiological characterization of different types of neurons recorded in vivo in the motor cortex of the cat. II. Membrane parameters, action potentials, current-induced voltage responses and electronic structures. J Neurophysiol. 69:1865–1879.

Branchereau P, Van Bockstaele EJ, Chan J, Pickel VM. 1996. Pyramidal neurons in rat prefrontal cortex show a complex synaptic response to single electrical stimulation of the locus coeruleus region: evidence for antidromic activation and GABAergic inhibition using in vivo intracellular recording and electron microscopy. Synapse. 22:313–331.

Chagnac-Amitai Y, Luhmann HJ, Prince DA. 1990. Burst generating and regular spiking layer 5 pyramidal neurons of rat neocortex have different morphological features. J Comp Neurol. 296:598–613.

Conde F, Maire-Lepoivre E, Audinat E, Crepel F. 1995. Afferent connections of the medial frontal cortex of the rat 2: Cortical and subcortical afferents. J Comp Neurol. 352:567–593.

Connors BW, Gutnick MJ, Prince DA. 1982. Electrophysiological properties of neocortical neurons in vitro. J Neurophysiol. 48:1302–1320.

Connors BW, Malenka RC, Silva LR. 1988. Two inhibitory postsynaptic potentials, and GABAA and GABAB receptor-mediated responses in neocortex of rat and cat. J Physiol. 406:443–468.

Contreras D, Timofeev I, Steriade M. 1996. Mechanisms of long-lasting hyperpolarizations underlying slow sleep oscillations in cat corticothalamic networks. J Physiol. 494:251–264.

Cossart R, Aronov D, Yuste R. 2003. Attractor dynamics of network UP states in the neocortex. Nature. 423:283–288.

Cowan RL, Wilson CJ. 1994. Spontaneous firing patterns and axonal projections of single corticostriatal neurons in the rat medial agranular cortex. J Neurophysiol. 71:17–32.

Crochet S, Chauvette S, Boucetta S, Timofeev I. 2005. Modulation of synaptic transmission in neocortex by network activities. Eur J Neurosci. 21:1030–1044.

Cunningham MO, Pervouchine DD, Racca C, Kopell NJ, Davies CH, Jones RS, Traub RD, Whittington MA. 2006. Neuronal metabolism governs cortical network response state. Proc Natl Acad Sci USA. 103:5597–5601.

D'Antuono M, Inaba Y, Biagini G, D'Arcangelo G, Tancredi V, Avoli M. 2006. Synaptic hyperexcitability of deep layer neocortical cells in a genetic model of absence seizures. Genes Brain Behav. 5:73–84.

Dash PK, Moore AN, Kobori N, Runyan JD. 2007. Molecular activity underlying working memory. Learn Mem. 14:554–563.

de la Pena E, Geijo-Barrientos E. 1996. Laminar localization, morphology, and physiological properties of pyramidal neurons that have the low-threshold calcium current in the guinea-pig medial frontal cortex. J Neurosci. 16:5301–5311.

DeFelipe J, Elston GN, Fujita I, Fuster J, Harrison KH, Hof PR, Kawaguchi Y, Martin KA, Rockland KS, Thomson AM, et al. 2002. Neocortical circuits: evolutionary aspects and specificity versus non-specificity of synaptic connections. Remarks, main conclusions and general comments and discussion. J Neurocytol. 31:387–416.

Degenetais E, Thierry AM, Glowinski J, Gioanni Y. 2002. Electrophysiological properties of pyramidal neurons in the rat prefrontal cortex: an in vivo intracellular recording study. Cereb Cortex. 12:1–16.

Degenetais E, Thierry AM, Glowinski J, Gioanni Y. 2003. Synaptic influence of hippocampus on pyramidal cells of the rat prefrontal cortex: an in vivo intracellular recording study. Cereb Cortex. 13:782–792.

Deisz RA, Prince DA. 1989. Frequency-dependent depression of inhibition in guinea-pig neocortex in vitro by GABAB receptor feed-back on GABA release. J Physiol. 412:513–541.
Delatour B, Witter MP. 2002. Projections from the parahippocampal region to the prefrontal cortex in the rat: evidence of multiple pathways. Eur J Neurosci. 15:1400–1407.
Destexhe A, Pare D. 1999. Impact of network activity on the integrative properties of neocortical pyramidal neurons in vivo. J Neurophysiol. 81:1531–1547.
Destexhe A, Rudolph M, Fellous JM, Sejnowski TJ. 2001. Fluctuating synaptic conductances recreate in vivo-like activity in neocortical neurons. Neuroscience. 107:13–24.
Floresco SB, Grace AA. 2003. Gating of hippocampal-evoked activity in prefrontal cortical neurons by inputs from the mediodorsal thalamus and ventral tegmental area. J Neurosci. 23:3930–3943.
Floresco SB, Tse MT. 2007. Dopaminergic regulation of inhibitory and excitatory transmission in the basolateral amygdala-prefrontal cortical pathway. J Neurosci. 27:2045–2057.
Fusi S, Drew PJ, Abbott LF. 2005. Cascade models of synaptically stored memories. Neuron. 45:599–611.
Gabbott P, Headlam A, Busby S. 2002. Morphological evidence that CA1 hippocampal afferents monosynaptically innervate PV-containing neurons and NADPH-diaphorase reactive cells in the medial prefrontal cortex (Areas 25/32) of the rat. Brain Res. 946:314–322.
Gabbott PL, Warner TA, Jays PR, Salway P, Busby SJ. 2005. Prefrontal cortex in the rat: projections to subcortical autonomic, motor, and limbic centers. J Comp Neurol. 492:145–177.
Gabel LA, Nisenbaum ES. 1998. Biophysical characterization and functional consequences of a slowly inactivating potassium current in neostriatal neurons. J Neurophysiol. 79:1989–2002.
Goldman-Rakic PS. 1995. Cellular basis of working memory. Neuron. 14:477–485.
Goto Y, Grace AA. 2005. Dopaminergic modulation of limbic and cortical drive of nucleus accumbens in goal-directed behavior. Nat Neurosci. 8:805–812.
Goto Y, Grace AA. 2006. Alterations in medial prefrontal cortical activity and plasticity in rats with disruption of cortical development. Biol Psychiatry. 60:1259–1267.
Hablitz JJ, Sutor B. 1990. Excitatory postsynaptic potentials in rat neocortical neurons in vitro. III. Effects of a quinoxalinedione non-NMDA receptor antagonist. J Neurophysiol. 64:1282–1290.
Hagenston AM, Fitzpatrick JS, Yeckel MF. 2008. MGluR-mediated calcium waves that invade the soma regulate firing in layer V medial prefrontal cortical pyramidal neurons. Cereb Cortex. 18:407–423.
Hasselmo ME. 2005. What is the function of hippocampal theta rhythm?—Linking behavioral data to phasic properties of field potential and unit recording data. Hippocampus. 15:936–949.
Herman JP, Prewitt CM, Cullinan WE. 1996. Neuronal circuit regulation of the hypothalamo-pituitary-adrenocortical stress axis. Crit Rev Neurobiol. 10:371–394.
Horvitz JC. 2000. Mesolimbocortical and nigrostriatal dopamine responses to salient non-reward events. Neuroscience. 96:651–656.
Howe JR, Sutor B, Zieglgansberger W. 1987. Characteristics of long-duration inhibitory postsynaptic potentials in rat neocortical neurons in vitro. Cell Mol Neurobiol. 7:1–18.
Insausti R, Herrero MT, Witter MP. 1997. Entorhinal cortex of the rat: cytoarchitectonic subdivisions and the origin and distribution of cortical efferents. Hippocampus. 7:146–183.
Ishikawa A, Nakamura S. 2003. Convergence and interaction of hippocampal and amygdalar projections within the prefrontal cortex in the rat. J Neurosci. 23:9987–9995.
Isomura Y, Sirota A, Ozen S, Montgomery S, Mizuseki K, Henze DA, Buzsaki G. 2006. Integration and segregation of activity in entorhinal-hippocampal subregions by neocortical slow oscillations. Neuron. 52:871–882[see comment].
Jay TM, Glowinski J, Thierry AM. 1989. Selectivity of the hippocampal projection to the prelimbic area of the prefrontal cortex in the rat. Brain Res. 505:337–340.
Jay TM, Witter MP. 1991. Distribution of hippocampal CA1 and subicular efferents in the prefrontal cortex of the rat studied by means of anterograde transport of Phaseolus vulgaris-leucoagglutinin. J Comp Neurol. 313:574–586.
Jung MW, Qin Y, McNaughton BL, Barnes CA. 1998. Firing characteristics of deep layer neurons in prefrontal cortex in rats performing spatial working memory tasks. Cereb Cortex. 8:437–450.
Kalus P, Slotboom J, Gallinat J, Federspiel A, Gralla J, Remonda L, Strik WK, Schroth G, Kiefer C. 2005. New evidence for involvement of the entorhinal region in schizophrenia: a combined MRI volumetric and DTI study. Neuroimage. 24:1122–1129.
Karlsson G, Pozza M, Olpe HR. 1988. Phaclofen: a GABAB blocker reduces long-duration inhibition in the neocortex. Eur J Pharmacol. 148:485–486[Erratum appears in Eur J Pharmacol. 1988 Sep 23;154(3):352].
Kawashima H, Izaki Y, Grace AA, Takita M. 2006. Cooperativity between hippocampal-prefrontal short-term plasticity through associative long-term potentiation. Brain Res. 1109:37–44.
Kelly JS, Krnjevic K. 1969. The action of glycine on cortical neurones. Exp Brain Res. 9:155–163.
Kerr JN, Greenberg D, Helmchen F. 2005. Imaging input and output of neocortical networks in vivo. Proc Natl Acad Sci USA. 102:14063–14068[see comment].
Kesner RP, Rogers J. 2004. An analysis of independence and interactions of brain substrates that subserve multiple attributes, memory systems, and underlying processes. Neurobiol Learn Mem. 82:199–215.
Komatsu Y, Nakajima S, Toyama K. 1991. Induction of long-term potentiation without participation of N-methyl-D-aspartate receptors in kitten visual cortex. J Neurophysiol. 65:20–32.
LaBar KS, Cabeza R. 2006. Cognitive neuroscience of emotional memory. Nat Rev Neurosci. 7:54–64.
Laroche S, Davis S, Jay TM. 2000. Plasticity at hippocampal to prefrontal cortex synapses: dual roles in working memory and consolidation. Hippocampus. 10:438–446.
Laroche S, Jay TM, Thierry AM. 1990. Long-term potentiation in the prefrontal cortex following stimulation of the hippocampal CA1/subicular region. Neurosci Lett. 114:184–190.
Lavin A, Grace AA. 2001. Stimulation of D1-type dopamine receptors enhances excitability in prefrontal cortical pyramidal neurons in a state-dependent manner. Neuroscience. 104:335–346.
Laviolette SR, Lipski WJ, Grace AA. 2005. A subpopulation of neurons in the medial prefrontal cortex encodes emotional learning with burst and frequency codes through a dopamine D4 receptor-dependent basolateral amygdala input. J Neurosci. 25:6066–6075.
Lewis BL, O'Donnell P. 2000. Ventral tegmental area afferents to the prefrontal cortex maintain membrane potential 'up' states in pyramidal neurons via D(1) dopamine receptors. Cereb Cortex. 10:1168–1175.
McCormick DA, Shu Y, Hasenstaub A, Sanchez-Vives M, Badoual M, Bal T. 2003. Persistent cortical activity: mechanisms of generation and effects on neuronal excitability. Cereb Cortex. 13:1219–1231.
McCracken CB, Grace AA. 2007. High-frequency deep brain stimulation of the nucleus accumbens region suppresses neuronal activity and selectively modulates afferent drive in rat orbitofrontal cortex in vivo. J Neurosci. 27:12601–12610.
McDonald RJ, Devan BD, Hong NS. 2004. Multiple memory systems: the power of interactions. Neurobiol Learn Mem. 82:333–346.
Meunier M, Cirilli L, Bachevalier J. 2006. Responses to affective stimuli in monkeys with entorhinal or perirhinal cortex lesions. J Neurosci. 26:7718–7722.
Nasrallah HA, Sharma S, Olson SC. 1997. The volume of the entorhinal cortex in schizophrenia: a controlled MRI study. Prog Neuropsychopharmacol Biol Psychiatry. 21:1317–1322.
Nunez A, Amzica F, Steriade M. 1993. Electrophysiology of cat association cortical cells in vivo: intrinsic properties and synaptic responses. J Neurophysiol. 70:418–430.
O'Donnell P, Grace AA. 1995. Synaptic interactions among excitatory afferents to nucleus accumbens neurons: hippocampal gating of prefrontal cortical input. J Neurosci. 15:3622–3639.
O'Donnell P, Lewis BL, Weinberger DR, Lipska BK. 2002. Neonatal hippocampal damage alters electrophysiological properties of prefrontal cortical neurons in adult rats. Cereb Cortex. 12:975–982.

Onn SP, Wang XB. 2005. Differential modulation of anterior cingulate cortical activity by afferents from ventral tegmental area and mediodorsal thalamus. Eur J Neurosci. 21:2975–2992.
Paxinos G, Watson C. 2007. The rat brain in stereotaxic coordinates. 6th ed. San Diego (CA): Academic Press.
Petersen CC, Hahn TT, Mehta M, Grinvald A, Sakmann B. 2003. Interaction of sensory responses with spontaneous depolarization in layer 2/3 barrel cortex. Proc Natl Acad Sci USA. 100:13638–13643.
Quirk GJ, Garcia R, Gonzalez-Lima F. 2006. Prefrontal mechanisms in extinction of conditioned fear. Biol Psychiatry. 60:337–343.
Ridderinkhof KR, Ullsperger M, Crone EA, Nieuwenhuis S. 2004. The role of the medial frontal cortex in cognitive control. Science. 306:443–447.
Rosenkranz JA, Moore H, Grace AA. 2003. The prefrontal cortex regulates lateral amygdala neuronal plasticity and responses to previously conditioned stimuli. J Neurosci. 23:11054–11064.
Sakagami M, Pan X. 2007. Functional role of the ventrolateral prefrontal cortex in decision making. Curr Opin Neurobiol. 17:228–233.
Sanchez-Vives MV, McCormick DA. 2000. Cellular and network mechanisms of rhythmic recurrent activity in neocortex. Nat Neurosci. 3:1027–1034.
Sarter M, Markowitsch HJ. 1985. Convergence of intra- and interhemispheric cortical afferents: lack of collateralization and evidence for a subrhinal cell group projecting heterotopically. J Comp Neurol. 236:283–296.
Sesack SR, Deutch AY, Roth RH, Bunney BS. 1989. Topographical organization of the efferent projections of the medial prefrontal cortex in the rat: an anterograde tract-tracing study with Phaseolus vulgaris leucoagglutinin. J Comp Neurol. 290:213–242.
Shu Y, Hasenstaub A, Badoual M, Bal T, McCormick DA. 2003. Barrages of synaptic activity control the gain and sensitivity of cortical neurons. J Neurosci. 23:10388–10401.
Simons JS, Spiers HJ. 2003. Prefrontal and medial temporal lobe interactions in long-term memory. Nat Rev Neurosci. 4:637–648.
Sotres-Bayon F, Cain CK, LeDoux JE. 2006. Brain mechanisms of fear extinction: historical perspectives on the contribution of prefrontal cortex. Biol Psychiatry. 60:329–336.
Steriade M, Nunez A, Amzica F. 1993a. Intracellular analysis of relations between the slow (< 1 Hz) neocortical oscillation and other sleep rhythms of the electroencephalogram. J Neurosci. 13:3266–3283.
Steriade M, Nunez A, Amzica F. 1993b. A novel slow (<1 Hz) oscillation of neocortical neurons in vivo: depolarizing and hyperpolarizing components. J Neurosci. 13:3252–3265.
Steriade M, Timofeev I, Grenier F. 2001. Natural waking and sleep states: a view from inside neocortical neurons. J Neurophysiol. 85:1969–1985.
Sutor B, Hablitz JJ. 1989. EPSPs in rat neocortical neurons in vitro. I. Electrophysiological evidence for two distinct EPSPs. J Neurophysiol. 61:607–620.
Swanson LW, Kohler C. 1986. Anatomical evidence for direct projections from the entorhinal area to the entire cortical mantle in the rat. J Neurosci. 6:3010–3023.
Szente MB, Baranyi A, Woody CD. 1988. Intracellular injection of apamin reduces a slow potassium current mediating afterhyperpolarizations and IPSPs in neocortical neurons of cats. Brain Res. 461:64–74.
Tierney PL, Degenetais E, Thierry AM, Glowinski J, Gioanni Y. 2004. Influence of the hippocampus on interneurons of the rat prefrontal cortex. Eur J Neurosci. 20:514–524.
Timofeev I, Grenier F, Steriade M. 2001. Disfacilitation and active inhibition in the neocortex during the natural sleep-wake cycle: an intracellular study. Proc Natl Acad Sci USA. 98:1924–1929.
Tseng KY, Mallet N, Toreson KL, Le Moine C, Gonon F, O'Donnell P. 2006. Excitatory response of prefrontal cortical fast-spiking interneurons to ventral tegmental area stimulation in vivo. Synapse. 59:412–417.
Vertes RP. 2004. Differential projections of the infralimbic and prelimbic cortex in the rat. Synapse. 51:32–58.
Vertes RP. 2006. Interactions among the medial prefrontal cortex, hippocampus and midline thalamus in emotional and cognitive processing in the rat. Neuroscience. 142:1–20.
Wilson CJ, Kawaguchi Y. 1996. The origins of two-state spontaneous membrane potential fluctuations of neostriatal spiny neurons. J Neurosci. 16:2397–2410.
Witter MP, Moser EI. 2006. Spatial representation and the architecture of the entorhinal cortex. Trends Neurosci. 29:671–678.
Yang CR, Seamans JK, Gorelova N. 1996. Electrophysiological and morphological properties of layers V–VI principal pyramidal cells in rat prefrontal cortex in vitro. J Neurosci. 16:1904–1921.